약학박사학위논문

암 환경에서 자연살해 T 세포 활성에 의한 기능저하 CD8 T 세포의 기능 회복에 관한 연구

Studies on reinvigorating exhausted CD8 T cells in tumor by NKT cell activation

2018 년 8 월

서울대학교 대학원
분자의학 및 바이오 제약학과 면역학 전공
배 은 아

Abstract

Studies on reinvigorating exhausted CD8 T cells in tumor by NKT cell activation

Bae, Eun-ah

Laboratory of Immunology

Department of Molecular Medicine and Biopharmaceutical Sciences

The Graduate School

Seoul National University

Cancer immunotherapy using immune checkpoint inhibitors has emerged as one of the most effective treatments for cancer patients. PD-1 blockade, in particular, is a successful example of immune checkpoint blockades that provides long-term durable therapeutic effects in cancer patients with a wide spectrum of cancer types. Accumulating evidence suggests that anti-PD-1 therapy enhances anti-tumor immunity by reversing the function of exhausted T cells in the tumor environment. However, the responsiveness rate of cancer patients to anti-PD-1 therapy remains low, providing an urgent need for the optimization of anti-PD-1 therapy for improved cure of cancer patients.

In this study, I established an anti-PD-1-resistant mouse tumor model and showed that unresponsiveness to anti-PD-1 was associated with gradual increases in CD8 T cell exhaustion. I also showed that invariant natural killer T (*i*NKT) cell stimulation by its synthetic ligand, α-galactosylceramide (αGC), could enhance the anti-tumor effect in anti-PD-1-resistant tumor models by restoring the effector function of tumor antigen-specific exhausted CD8 T cells. Among the cytokines produced by αGC stimulation, IL-2 and IL-12 appeared to be crucial for reinvigorating exhausted CD8 T cells in tumor-bearing mice and cancer patients. Furthermore, combining αGC-loaded antigen-presenting cells and PD-1 blockade elicits the improved antitumor activities in therapeutic murine tumor models. Thus, this study suggests that NKT cell stimulation would be a promising therapeutic candidate for the treatment of anti-PD-1-resistant cancer in humans.

Keywords: CD8 T cell Exhaustion, Natural Killer T (NKT) cell, PD-1 Blockade, IL-2, IL-12, Cancer Immunotherapy

Student number: 2012-22844

Table of Contents

List of Figures and Tables

Abbreviations

Ab	Antibody
Ag	Antigen
APC	Antigen presenting cell
αGC	alpha galactosylceramide
CD	Cluster of differentiation
CTL	Cytotoxic T lymphocyte
DC	Dendritic cell
FACS	Fluorescence activated cell sorter
GrazB	Granzyme B
IFN-γ	Interferon-gamma
IL-	Interleukin-
i.p.	Intraperitoneally
i.v.	Intravenous
Mo	Monocyte
mAb	Monoclonal antibody
NKT	Natural Killer T
OVA	Ovalbumin
PBMC	Peripheral blood mononuclear cell

PD-1	Programmed cell death-1
RBC	Red blood cell
s.c.	Subcutaneously
TdLN	Tumor draining lymph node
TIL	Tumor-infiltrating lymphocyte
TNF-α	Tumor necrosis factor-alpha

Introduction

CD8 T cell exhaustion and anti-PD-1 therapy

CD8 T cells play a crucial role in eliminating abnormal cells in the body, including cancer cells **(Figure 1)**(1). However, prolonged exposure to antigen in the tumor microenvironment results in functional exhaustion of CD8 T cells, which is associated with the high expression levels of coinhibitory receptors such as programmed death-1 (PD-1, CD279), LAG-3 and Tim-3 (2-4). To reinvigorate the anti-tumor effector function of exhausted/dysfunctional CD8 T cells, immune checkpoint inhibitors targeting the coinhibitory receptors have been developed **(Figure 2)**(5-8) and have produced promising outcomes in clinical trials treating patients with melanoma, renal cell cancer and non-small-cell lung cancer (9-11). In addition, the combination of ipilimumab (anti-CTLA4) with nivolumab (anti-PD-1) for the treatment of advanced melanoma patients has resulted in more rapid and durable clinical responses with a manageable safety profile (12). However, not all cancer patients are readily responsive to immune checkpoint therapy, demonstrating an unmet need to optimize immune checkpoint blockade and combination therapies (9,13,14).

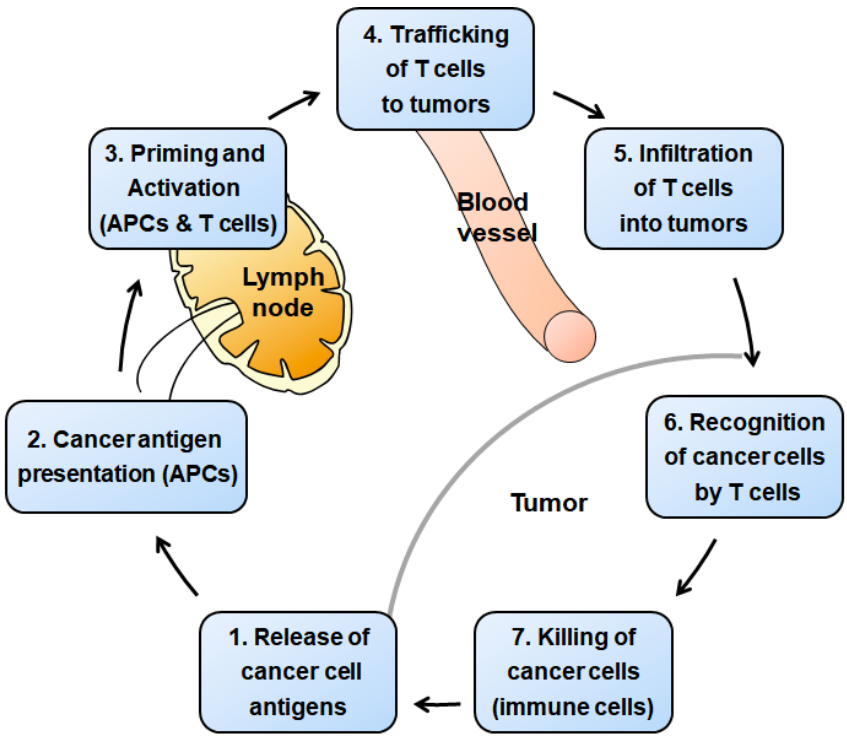

Figure 1. The immunity cycle against cancer

This cancer-immunity cycle consists of seven major steps and can be self-amplified by a cyclic loop. It begins with the release of cancer cell antigens from tumor. Antigen presenting cells could uptake and present cancer antigens to T cells in lymph nodes. Activated T cells could infiltrate the tumor and eliminate the cancer cells (1).

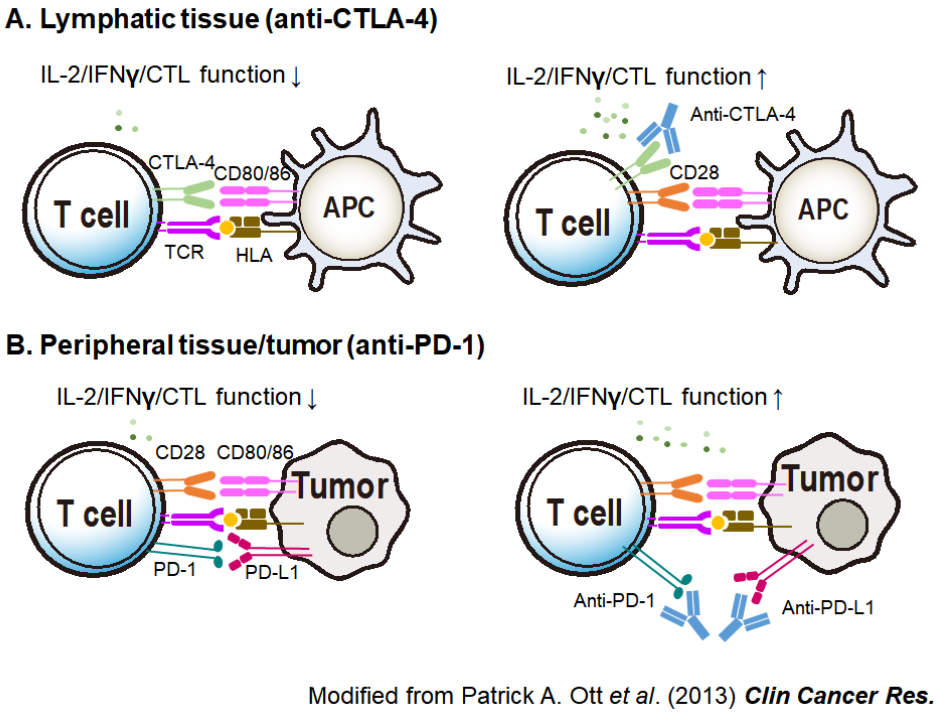

Modified from Patrick A. Ott *et al*. (2013) ***Clin Cancer Res.***

Figure 2. Mechanisms of immune checkpoint inhibitors

(A) CTLA-4 is upregulated in activated T cells and competes with the costimulatory molecule CD28 for binding its ligands B7.1/2 (CD80/CD86). As CTLA-4 has a higher binding affinity with its ligands, costimulatory signal is blocked and it leads to inhibition of the T cell activation and proliferation. CTLA-4 blockades could restore the effector function of T cells. **(B)** PD-1 is a coinhibitory molecule and interacts with its ligands B7-H1 and B7-DC (PD-L1 and PD-L2). PD-1 is upregulated on T cells in tumor and PD-1 signal leads to apoptosis and decrease in the effector function of T cells (8).

CD8 T cells and cytokines

To guarantee optimal activation of CD8 T cells, three independent signals are needed: TCR engagement (signal 1), co-stimulation (signal 2) and cytokines (signal 3) **(Figure 3)**(15,16). It has been suggested that these three different signals are also required for the functional recovery of exhausted T cells. For example, the CD28/B7 costimulatory pathway is essential for the functional restoration of exhausted CD8 T cells by anti-PD-1 therapy in the tumor or during chronic viral infection (17). In addition, several studies have shown that various cytokines, such as IL-2 or IL-12, are important for restoring the effector functions of exhausted CD8 T cells in chronic viral infection models (18,19). IL-21 is also required for CD8 T cell effector functions during chronic viral infection (20,21). Furthermore, dysfunctional CD8 T cells can be rescued and expanded by exogenous IL-15 (22).

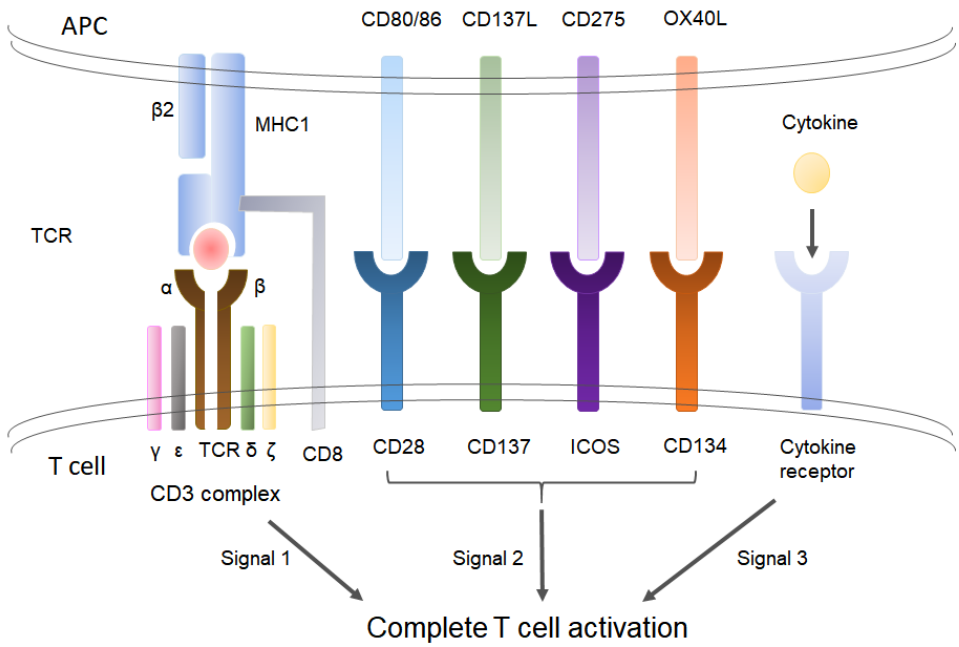

Modified from Michael H. Kershaw *et al.* (2013) ***Nature Reviews***

Figure 3. T cell activation by three signals

Naïve T cells can be initially activated by interaction of their T cell receptors with a peptide antigen-loaded on major histocompatibility complexes (MHC) in antigen-presenting cells (APCs) (signal 1). At the same time, co-stimulatory signals are required for the fully activated T cells (signal 2). Cytokine signals are also needed for further activation and proliferation (signal 3) (16).

NKT cells and their ligand, alpha-galactosylceramide (αGC)

Natural killer T (NKT) cells are a unique subset of T lymphocytes positioned at the border between the innate and adaptive immune system. Invariant NKT (*i*NKT) cells, which express an invariant TCR composed of Vα14-Jα18 chains in mice (Vα24-Jα18 in humans), constitute a major portion of NKT cells (23,24). Alpha-galactosylceramide (αGC) is a synthetic ligand for *i*NKT cells (24). Upon *in vivo* administration, αGC loaded onto CD1d, a non-classical class I-like molecule, expressed on antigen-presenting cells activates *i*NKT cells to rapidly produce various cytokines, including IFNγ, IL-4, IL-2, IL-10, and IL-21 (25-29), and also transactivates dendritic cells (DCs) to secrete IL-12 **(Figure 4)**(30-32). As *i*NKT cells can induce both innate and adaptive anti-tumor immunity, *i*NKT cell activation is one of the promising therapeutic approaches for cancer immunotherapy (33,34). While the direct administration of soluble αGC induces anergy of *i*NKT cells after a rapid production of cytokines, cell-associated αGC extends the duration of *i*NKT cell responses (35). In this regard, we have previously reported that αGC-loaded, antigenic peptide-pulsed B cells elicit a potent and long-lasting anti-tumor immunity (36,37).

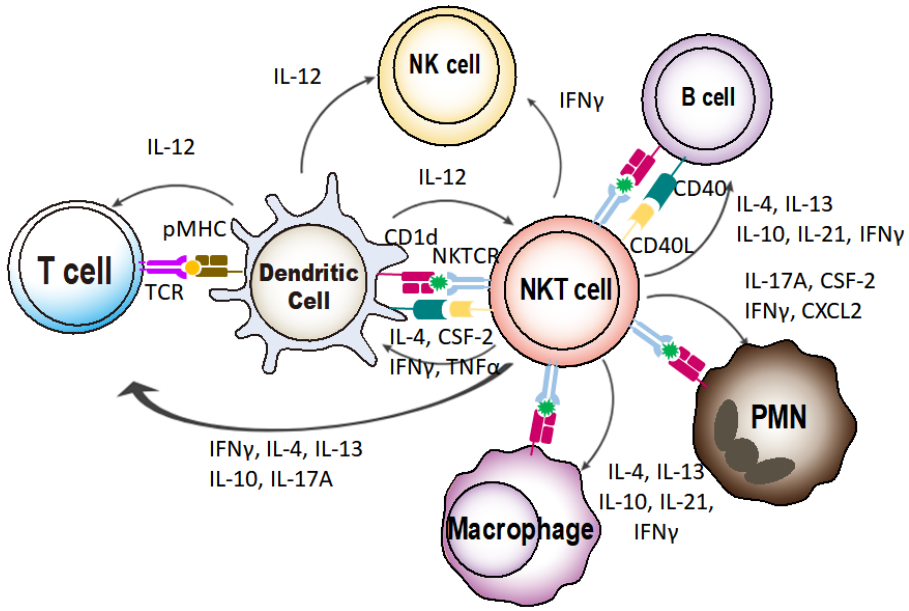

Modified from Amrendra Kumar *et al*. (2017) ***Front Immunol.***

Figure 4. The immunological functions of activated NKT cells

Activated *i*NKT cells can crosstalk with diverse immune cells. Upon activation by their ligands such as αGC *in vivo*, *i*NKT cells rapidly produce various cytokines and chemokines, which facilitate the differentiation of T cells into effector cells and the activation of antigen presenting cells. IL-12 secreted by matured dendritic cells, in turn, activates NK cells and T cells (29).

Purpose of this study

As B cells and monocytes (Mo) could also become immunogenic antigen-presenting cells (APCs) in response to activated *i*NKT cells (36,38), the B/Mo/αGC vaccine platform in which B cells and monocytes serve as professional APCs, and cell-associated αGC acts as an adjuvant has been established (39). A previous study has recently demonstrated that *i*NKT cell stimulation by αGC-loaded APCs can eradicate advanced tumors containing major histocompatibility complex (MHC) class I-deficient tumor cells by reinvigorating the effector function of NK cells (39). IL-21 produced by *i*NKT cells appeared to be responsible for the functional recovery of exhausted NK cells **(Figure 5)**(39,40). However, whether cytokines induced by the administration of αGC-loaded APCs can also restore the function of exhausted CD8 T cells in the tumor environment remains elusive.

In the present study, I aimed to evaluate the role of cytokines induced by αGC-loaded APCs on exhausted CD8 T cells in the tumors. I found that cytokines induced by *i*NKT cell activation, especially IL-2 and IL-12, could reverse the effector functions of exhausted CD8 T cells. In addition, I showed that the combination of αGC-loaded APCs and PD-1 blockade synergistically

augmented the anti-tumor effects in a mouse therapeutic tumor model. Collectively, I propose mechanistic insights into the efficacy of the combined treatment with αGC-loaded APCs and PD-1 blockades by showing that *i*NKT cell activation can overcome the exhausted phenotype of tumor-associated CD8 T cells via IL-2 and IL-12.

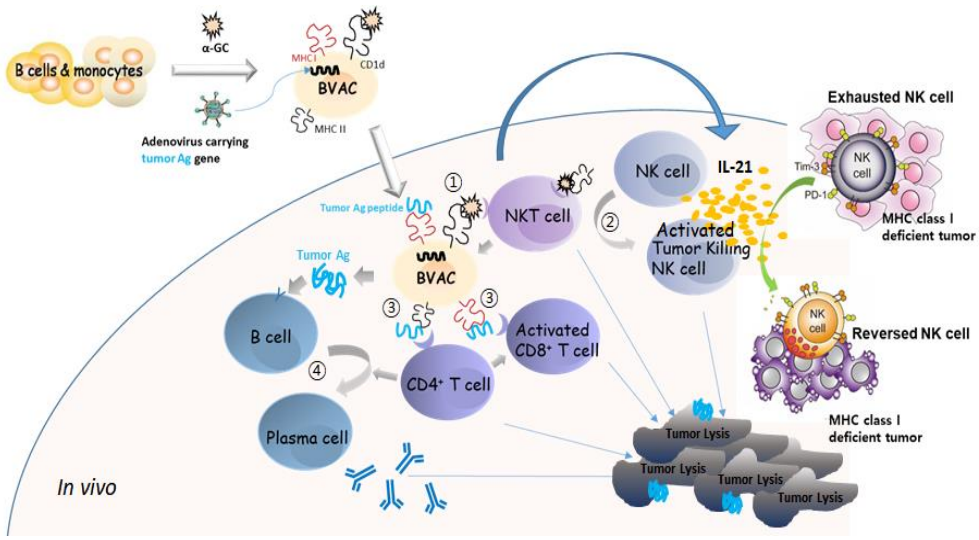

Figure 5. Mode of action of *i*NKT ligand loaded tumor Ag-expressing B cell- and monocyte-based vaccine. Our vaccine platform consists of an invariant natural killer T (*i*NKT) cell ligand, αGC, loaded on tumor antigen (tAg)-expressing B cells and monocytes (B/Mo/tAg/αGC). This vaccine (B/Mo/tAg/αGC) elicits a wide range of anti-tumor immune responses. αGC activates NKT cells (①) and activated NKT cells can trans-activate NK cells (②). Furthermore, tAg-expressing B cells and monocytes can induce tAg-specific CD4 and CD8 T cell responses (③). Simultaneously, this vaccine produces tumor Ag, which eventually could lead to Ag-specific Ab production (④). Moreover, IL-21 produced by *i*NKT cells induces the functional restoration of exhausted NK cells.

Materials and Methods

Mice

Female C57BL/6 and BALB/c mice were purchased from Charles River Laboratories (Seoul, Korea). OVA-specific T cell receptor transgenic OT-I mice (C57BL/6-Tg(TcraTcrb)1100Mjb/J) and CD45.1 congenic mice (B6.SJL-Ptprc^{a} Pepc^{b}/BoyJ) were purchased from the Jackson Laboratory. OT-I mice were crossed with CD45.1 mice to generate CD45.1^{+}OT- I mice. All mice were used at 6 to 12 weeks of age and were bred and maintained in the specific pathogen-free vivarium of Seoul National University. All animal experiments were approved by the Institutional Animal Care and Use Committee (IACUC; SNU-170117-2-1) at Seoul National University.

Human Samples

Human tumor tissue specimens from 11 colorectal cancer patients were collected at the Department of Surgery, Shinchon Severance Hospital, Yonsei University College of Medicine **(Table 1)**. Written informed consent was

obtained from the patients or their guardians. The tumor tissues were placed in in RPMI 1640 medium (Gibco) supplemented with 10% FBS (Gibco), 1% penicillin/streptomycin (Lonza), 1 mmol/L sodium pyruvate (Gibco), 0.1 mmol/L NEAA (Gibco), 55 mmol/L 2-mercaptoethanol (Gibco), and 25 mmol/L HEPES (Gibco) on ice before tumor dissociation. Single cell suspensions from tumors were rested and stimulated with recombinant human IL-2 (10 ng/mL; R&D Systems, Minneapolis, MN, USA, cat: 202-IL) and IL-12 (10 ng/mL; R&D Systems, cat: 219-IL) overnight. They were further restimulated with soluble anti-CD3 (1 μg/mL, OKT3; BioLegend, San Diego, CA, USA) in the presence of cytokines for 5h.

Human peripheral blood mononuclear cells (PBMCs) were obtained from 2 healthy donors in compliance with Institutional Review Board protocols, and informed consent was granted from all donors. The collection of human samples and all human experiments were performed in accordance with the principles of the Helsinki Declaration and approved by the ethical committee of Seoul National University and Shinchon Severance Hospital, Yonsei University College of Medicine (IRB No. 1712/001-003).

Tumor cell lines

B16F10-OVA cells (kindly provided by Dr. K. Rock, University of Massachusetts Medical School) were cultured in DMEM (Gibco) supplemented with 10% FBS, 1% penicillin-streptomycin, 200 μg/mL of geneticin (Gibco) and 60 μg/mL of hygromycin (Invitrogen). CT26 cells and MC38 cells (purchased from ATCC; CT26 was purchased in 2002, and MC38 was purchased in 2006) were cultured in DMEM with 10% FBS and 1% penicillin-streptomycin. Tumor cell lines were validated by morphology, growth kinetics, and antigen expression. The cells were distributed in several vials (1.0×10^6/vial) with culture media supplemented with 10% DMSO (Sigma-Aldrich, St. Louis, MO, USA) and stored in a liquid nitrogen tank. All cell lines were found to be negative for mycoplasma contamination, and these cell lines were used from passages 3 to 7 for all experiments.

For the *in vivo* transplant tumor models, B16F10-OVA cells (1.0×10^6 per mouse), MC38 (3.0×10^5 per mouse) and CT26 cells (3.0×10^5 per mouse) were subcutaneously (s.c.) injected into the left flank of female C57BL/6 mice and BALB/c mice respectively. Tumor growth was measured using a metric caliper 2-3 times a week. Tumor volume was calculated as 0.5236 ×

length × width × height as described previously (33). Mouse survival was examined by actual survival, and mouse whole tumor weight was measured by microbalance upon sacrifice on day 22 after tumor inoculation.

Preparation of αGC-cultured supernatant (αGC Sup)

Splenocytes isolated from C57BL/6 mice were homogenized using a 70-μm cell strainer (FALCON, USA), and red blood cells (RBC) were lysed using ACK lysing buffer (Gibco). Isolated total splenocytes (3.3×10^6/mL) were stimulated with αGC (200 ng/mL) (KRN7000, Enzo Life Science, Japan) or their vehicle DMSO as a control for 24 h. The αGC-cultured supernatant (αGC Sup) was collected and stored at -20°C. For B/Mo/αGC-stimulated culture supernatants, total splenocytes were cultured with αGC-loaded B/Mo or their vehicle-loaded B/Mo at 5:1 for 24 h. B/Mo/αGC Sup was also stored at -20℃ before use.

To make human αGC-cultured supernatant, PBMCs were prepared by density gradient centrifugation using Ficoll-Histopaque-1077 Hybri-Max™ (Sigma-Aldrich) as previously described (41). To enrich for *i*NKT cells, PBMCs were cultured with αGC for 7 days and then cultured for an additional 7-10 days in

the presence of recombinant human IL-2 (200 U/mL). Cultured *i*NKT cells were purified with anti-human *i*NKT microbeads (Miltenyi Biotec, Bergisch Gladbach, Germany). To prepare αGC-loaded APCs in humans, T cell-depleted PBMCs were incubated with αGC (1 μg/mL) or DMSO overnight. In a 96-well plate, 2.0×10^5 *i*NKT cells were stimulated with 1.0×10^6 αGC-loaded APCs for 24 h as previously demonstrated with some modifications (42). The resultant human αGC-cultured supernatant (αGC Sup) was stored at -20℃ before use.

Preparation of αGC-loaded APC (B/Mo/αGC)

Splenocytes were isolated from C57BL/6 or BALB/c mice. After eliminating RBCs using ACK lysing buffer, the $CD11b^+$ cells and $B220^+$ cells were purified using anti-mouse CD11b and anti-mouse B220 microbeads (all from Miltenyi Biotec). Isolated B cells and monocytes (Mo) were incubated with αGC (1 μg/mL) or their vehicle DMSO for 18 h based on our previous studies (36-39,43-45).

Isolation and activation of Ag-specific CD8 T cells

Total CD8 T cells isolated from the spleen and lymph nodes of OT-I mice by positive selection using anti-mouse CD8 microbeads (Miltenyi Biotec, 2.43) were activated by anti-CD3 (clone 145-2C11) and anti-CD28 (clone 37.51) (BioLegend) at 1 μg/mL on pre-coated plates based on previous studies (46). On day 2, T cells were harvested from the antibody-coated plate and amplified with low dose recombinant IL-2 (Peprotech, Rocky Hill, NJ, USA cat: 212-12) until day 5, when the cells were adoptively transferred into tumor-bearing mice.

Adoptive T cell transfer and antibody treatments in the B16F10-OVA tumor model

CD45.1^{+}OT-I CD8 T cells generated *in vitro* were transferred by intravenous (i.v.) injection (2-3 × 10^6 per mouse) into the tumor-bearing mice 12 days after B16F10-OVA tumor inoculation. For ex-vivo analyses, mice were sacrificed on day 8 after adoptive T cell transfer, and T cells in the tumor were isolated as described in the section on tumor-infiltrating lymphocyte preparation. To identify *in vivo* effects of αGC, 8 days after adoptive T cell transfer, 2.0 × 10^6 B cells and monocytes loaded with αGC (B/Mo/αGC) or

their control-loaded B/Mo were transferred into the tumor-bearing mice by i.v. injection. The mice were sacrificed 2 days after B/Mo/αGC transfer.

In selected experiments, to deplete CD8 T cells, 300 μg of anti-CD8 (2.43, cat: BE0061) or control antibody was injected intraperitoneally (i.p.) every 3 days into the mice, beginning on the day before B/Mo/αGC transfer. To neutralize IL-2 and IL-12, anti-IL-2 (JES6-5H4, cat: BE0042), anti-IL-12p40 (C17.8, cat: BE0051) or both were i.p. injected (1 mg/mouse) 2 h before the B/Mo/αGC transfer, and then 24, 48 h after the first injection (500 μg/mouse).

In combined therapy experiments, B/Mo/αGC was injected intravenously. when the tumor size was greater than 200 mm^3 and 300 μg of anti-PD-1 (RMP1-14, cat: BE0146) treatment was i.p. administered every 3 days beginning on the same day as B/Mo/αGC. The antibodies for *in vivo* depletion (CD8, IL-2, IL-12p40, PD-1 and control antibodies) were purchased from BioXcell (USA).

Preparation of tumor-infiltrating lymphocyte

Tumor tissues from mice and patients were cut into small pieces (approximately 2 to 5 mm) and dissociated in C tubes using the gentleMACS

Dissociator (Miltenyi Biotec). Single cell suspensions from dissociated mouse tumor samples were prepared as previously described with minor modifications (40,47). Briefly, tumors were digested in 2% FBS with RPMI medium containing 1 mg/mL collagenase D (Roche), 100 μg/mL hyaluronidase (Sigma Aldrich) and 100 μg/mL DNase I (Sigma Aldrich) at 37℃ for 30 min, followed by lymphocyte isolation using lymphocyte separation medium (MP Biomedicals, cat: 0850494). The patient tumor samples were digested with the tumor dissociation kit containing enzyme A, H and R (Miltenyi Biotec, cat: 130-095-929) at 37°C using the manufacturer's recommended instructions. After dissociation, single cell suspensions were filtered through a 70-μm cell strainer and used for the experiments.

Flow cytometry analysis

CD8 T cells were isolated from tumor-infiltrating lymphocytes using anti-mouse CD8 microbeads (Miltenyi Biotec) with a MACS LS column (Miltenyi Biotec). Isolated tumor-infiltrating CD8 T cells were stimulated with αGC Sup (containing 50%) and T-cell-depleted APCs loaded with OT-I peptide (SIINFEKL, 257-264; AnaSPEC) for 3 days. T cell-depleted APCs were generated by CD3 depletion as described previously (48). Briefly,

splenocytes were stained with biotinylated anti-CD3 mAb (Biolegend) and anti-biotin microbeads (Miltenyi Biotec), after which a MACS LD column (Miltenyi Biotec) was used. In a selected experiment, $CD38^{hi}CD101^{hi}$ and $CD38^{low}CD101^{low}$ $CD45.1^{+}$ CD8 T cells were further sorted using a FACSAIRA II at the National Center for Inter-University Research Facilities (NCIRF) at Seoul National University.

The cells (mouse and human primary cells: 1.0×10^5 to 1.0×10^6) were stained with the specified antibodies in FACS buffer (PBSN+1% FBS). For intracellular cytokine staining, CD8 T cells were restimulated with brefeldin A (GolgiPlug; BD Biosciences, San Jose, CA, USA) and monensin (GolgiStop; BD Biosciences) for the last 4 h, followed by fixation and permeabilization using the Cytofix-Cytoperm kit (BD Biosciences). A phycoerythrin-conjugated CD107a antibody (1D4B; BioLegend, cat:1216) was added during cell restimulation. For transcription factor staining, cells were permeabilized with the Foxp3 staining kit (eBioscience, San Diego, CA, USA) according to the manufacturer's instructions.

The antibodies against mouse PD-1 (RMP1-30, cat: 1091), Tim3 (RMT3-23, cat: 1197), LAG3 (C9B7W, cat: 1252), CD3ε (145-2C11, cat: 1003), CD8α (53-6.7, cat: 1007), TNFα (MP6-XT22, cat: 5063), granzyme B (GB11, cat:

5154), CD44 (IM7, cat: 1030), CD28 (37.51, cat: 1021), CD38 (90, cat: 1027), ki67 (16A8, cat: 6524), CD45.2 (104, cat: 1098), CD45.1 (A20, cat: 1107), CD69 (H1.2F3, cat: 1045), B220 (RA3-6B2, cat: 1032) CD11b (M1/70, cat: 1012), CD11c (N418, cat: 1173), and IL-2 (JES6-5H4, cat: 5038) were purchased from Biolegend. The antibody against mouse IL-12 (p40/p70) (C45.6, cat: 554479) was purchased from BD Biosciences. The antibodies against mouse IFNγ (XMG1.2, cat: 7311), PD-1 (J43, cat: 9985), CD101 (Moushi101, cat: 1011), T-bet (4B10, cat: 5825), and human IFNγ (4S.B3, cat: 7319) were purchased from eBioscience. The antibodies against human CD45 (2D1, cat: 3685), CD3 (SK7, cat: 3448), CD8α (RPA-T8, cat: 3010), and TNFα (MAB11, cat: 5029) were purchased from Biolegend. All antibodies were used at a concentration of 2 μg/mL except for the FITC-conjugated antibodies, which were used at 5 μg/mL. The cells were incubated at 4℃ in the dark for 15 minutes and then were washed with FACS buffer. Dead cells were excluded by staining with the Fixable Violet Dead cell kit (Molecular Probes™, Invitrogen, Eugene, OR, USA) or Fixable Viability Dye (eBioscience) following the manufacturers' instructions. Intracellular staining was performed for 30 minutes after fixation and permeabilization according to the manufacturer's instructions. The samples were analyzed with

a FACSAria III or LSRFortessa X-20 instrument (BD Biosciences), and the data were analyzed with FlowJo software (Tree Star). Tumor-infiltrating CD45.1^{+}OT-I cells were calculated as follows:

$$(= \frac{\%\ of\ \text{CD45.1}^{+}\text{OT-I cells} \times \text{No. of tumor-infiltrating lymphocytes}}{tumor\ weight\ (mg)}).$$

In vitro **cytotoxicity assay**

Effector CD8 T cells were prepared from the tumor-bearing mice which had been transferred with CD45.1^{+}OT-I cells and B/Mo/αGC. CD8 T cells were isolated from tumor-infiltrating lymphocytes using anti-mouse CD8 microbeads (Miltenyi Biotec, Bergish Galdbach, Germany) and used to further sort CD45.1^{+} populations using a FACSARIA III (BD Biosciences). Target cells were B16F10-OVA cells that had been cultured in the presence of murine recombinant IFNγ (10 ng/mL, R&D Systems) for 24 h to induce increased expression of MHC class I. CD45.1^{+}CD8 T cells were cocultured with ^{51}Cr-labeled B16F10-OVA tumor cells for 4-5 h. The effector-to-target cell ratios (E:T) were 3:1 and 20:1, and the CTL activity was calculated by the release of ^{51}Cr into the culture supernatants via the specific lysis of B16F10-OVA target cells, which was measured using a Wallac 1470 Wizard

automatic γ-counter (PerkinElmer, USA). Specific lysis (%) was calculated as follows:

$[\% = \frac{(\text{Experimental release} - \text{Spontaneous release})}{(\text{Maximum release} - \text{Spontaneous release})} \times 100]$ as previously described (44).

Statistics

Statistical comparisons were performed using Prism 6.0 software (GraphPad Software). In experiments with mice, an unpaired two-tailed Student *t*-test was used to compare two groups. Two-way ANOVA with Bonferroni multiple comparisons test was used for multiple comparisons. A log-rank (Mantel-Cox) test (conservative) was used to analyze tumor survival. For human samples, the paired Student *t*-test was used. P values <0.05 were considered statistically significant.

Results

Administration of αGC-loaded APCs inhibits tumor growth in an anti-PD-1-resistant tumor model.

To investigate the effects of PD-1 blockade on exhausted CD8 T cells in tumors, I analyzed the PD-1 expression from the mice bearing B16F10-OVA, a murine melanoma cell line expressing the exogenous antigen ovalbumin (OVA). As previously shown by others, the cell surface expression of PD-1 in tumor-infiltrating CD8 T cells gradually increased with tumor progression, whereas that in tumor-draining lymph nodes (TdLNs) was not up-regulated **(Figure 6A-B)** (2,46,49). Of note, anti-PD-1 antibody treatment eradicated tumors if administered at the early stage of tumor progression when the tumor was palpable (anti-PD-1 working model); however, tumor growth was not controlled by the treatment of anti-PD-1 at the later time points when the tumor size was approximately 200 mm^3 (anti-PD-1-resistant model) **(Figure 7A-C)**. Previous study showed that the αGC-loaded, tumor-antigen-expressing APC-based vaccine could eradicate advanced tumors (39). Thus, I examined whether treatment with αGC-loaded B cells and monocytes

(αGC-loaded APCs) could induce anti-tumor responses in the anti-PD-1-resistant model. The administration of αGC-loaded APCs significantly inhibited tumor growth, which was accompanied by the increase in overall survival rates **(Figure 7D-F)**. I also observed comparable *i*NKT cell activation and tumor regression with intravenous injection of αGC **(Figure 8A-B)**. The activation status of *i*NKT cells in the tumor site was not changed with αGC treatment regardless of the delivery system, although intravenous injection of αGC more effectively expanded *i*NKT cells in the spleen than αGC-loaded APC administration **(Figure 8B-C)**. Tumor growth in another anti-PD-1-resistant tumor model was also inhibited by the treatment of αGC-loaded APCs **(Figure 9)**. Furthermore, I found that depletion of CD8 T cells significantly reversed the inhibition of tumor growth, implying that anti-tumor immunity mediated by the treatment of αGC-loaded APCs was dependent on CD8 T cells **(Figure 7E-F)**.

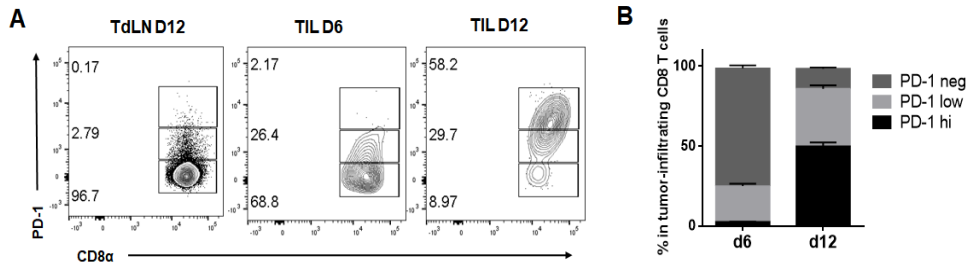

Figure 6. PD-1 expression is upregulated in tumor-infiltrating CD8 T cells.

(A-B) C57BL/6 mice were s.c. injected with B16F10-OVA. CD8 T cells were obtained from tumors and tumor-draining LNs (TdLNs) on the indicated days after tumor inoculation. Representative flow cytometry plots and graphs show the intensity of PD-1 expression. Data are representative of two or more independent experiments.

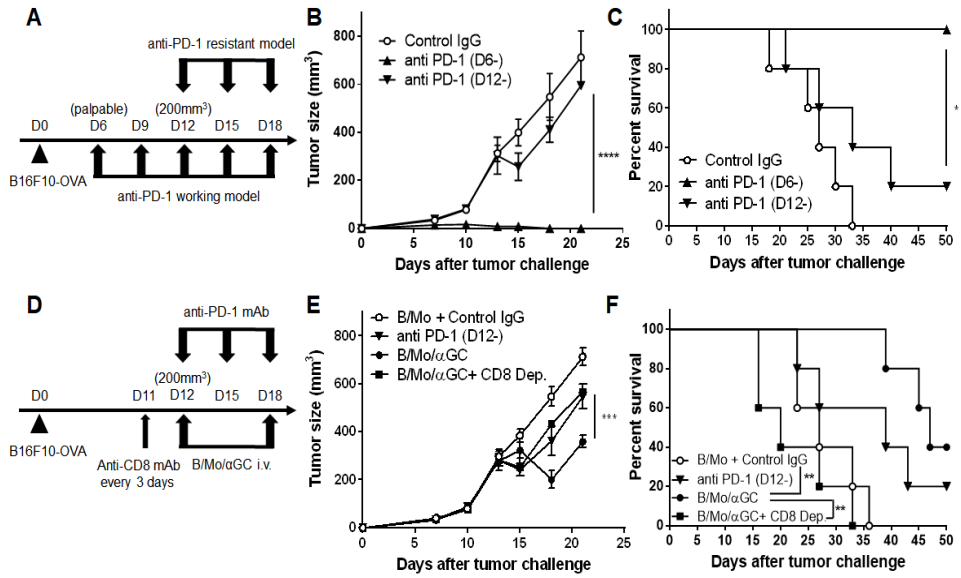

Figure 7. Administration of αGC-loaded APCs inhibits tumor growth in an anti-PD-1-resistant tumor model.

(A-C) B16F10-OVA-bearing mice were treated with 300 µg of control IgG or anti-PD-1 on days 6, 9, 12, 15, and 18 (anti-PD-1 working model) or on days 12, 15, and 18 (anti-PD-1-resistant model). **(D-F)** B16F10-OVA-bearing mice were treated with control IgG or anti-PD-1 on days 12, 15, and 18 (anti-PD-1-resistant model) or injected with B/Mo/αGC or their control B/Mo on days 12 and 18. To deplete CD8 T cells, tumor-bearing mice were i.p. injected with anti-CD8 (2.43) every three days, starting on the day before initiation of the treatments. **(B and E)** Tumor growth was measured three times weekly, and tumor sizes are

presented as the means ± SEM. Statistical differences in tumor sizes were determined by two-way analysis of variance (ANOVA) with Bonferroni multiple comparison tests. **(C and F)** Survival curves from data in **(B** and **E)**. The data are representative of two independent experiments that included four to six mice per group. Comparisons were performed using the log-rank (Mantel-Cox) test (*, $P<0.05$; **, $P<0.01$; ***, $P<0.001$; ****, $P<0.0001$).

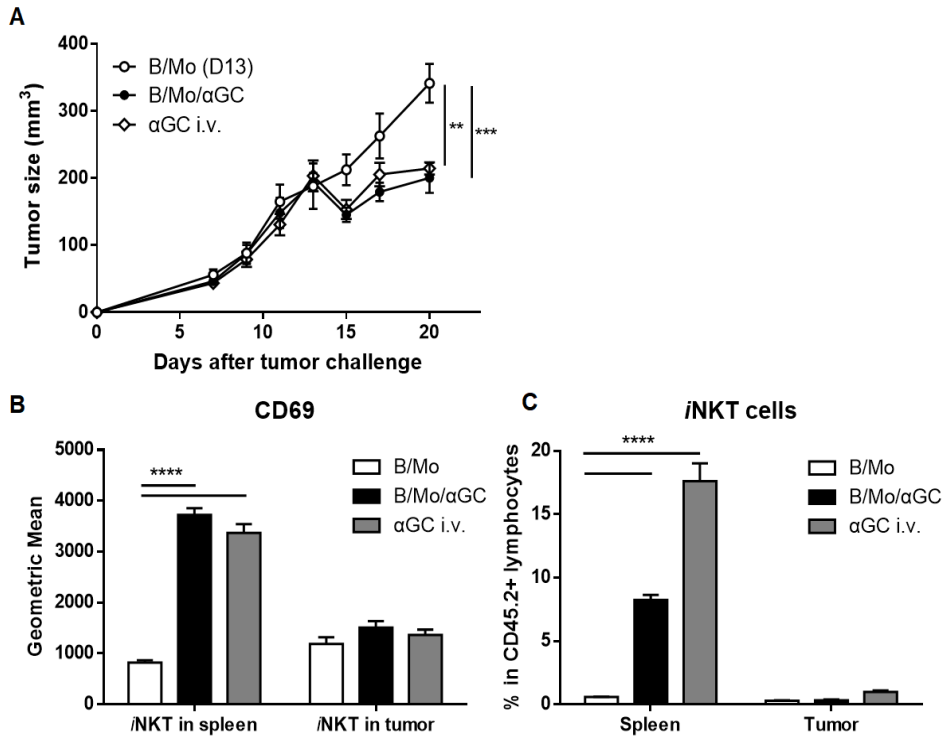

Figure 8. Administration of αGC-loaded APCs elicits similar antitumor immunity as αGC alone.

(A-C) C57BL/6 mice were s.c. injected with B16F10-OVA tumor cells (1.0×10^6). **(A)** Thirteen days after tumor cell implantation, when the average tumor size reached more than 200 mm^3, treatment began. Tumor-bearing mice were injected with B/Mo or B/Mo/αGC (2.0×10^6 each) or αGC (2 μg) intravenously. Tumor growth was monitored three times weekly, and tumor sizes are presented as the means ± SEM. **(B)** CD69 expression on *i*NKT cells was assessed 6 hours after

treatment. **(C)** The frequency of *i*NKT cells in the spleen and tumor was analyzed 3 days after treatment. The data are representative of two independent experiments (4-7 mice per group). The data in **(A-C)** were analyzed by two-way analysis of variance (ANOVA) with Bonferroni multiple comparison tests (*, $P<0.05$; **, $P<0.01$; ***, $P<0.001$).

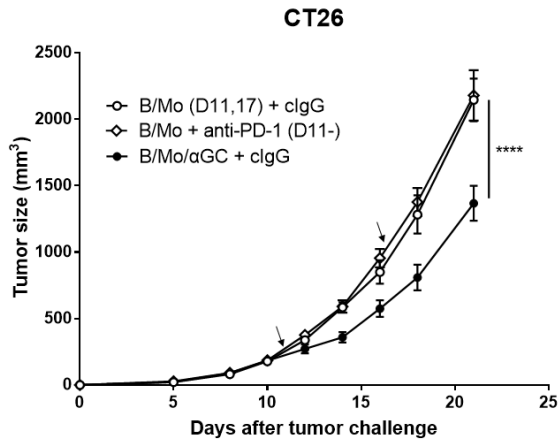

Figure 9. Administration of αGC-loaded APCs elicits tumor growth inhibition in the CT26 tumor model.

BALB/c mice were s.c. injected with CT26 tumor cells (3.0×10^5). Treatment began 11 days post-tumor inoculation when the average tumor size reached more than 200 mm^3. Tumor-bearing mice were treated with 300 μg of control IgG or anti-PD-1 on days 11, 14, 17, and 20 (anti-PD-1-resistant model) or injected with B/Mo or B/Mo/αGC on days 11 and 17. Tumor growth was monitored three times weekly, and tumor sizes are presented as the means ± SEM. The data show one representative experiment (4-7 mice per group) out of two independent experiments. Statistical differences in tumor sizes were determined by two-way ANOVA with Bonferroni multiple comparison tests (*, $P<0.05$; **, $P<0.01$; ***, $P<0.001$; ****, $P<0.0001$).

αGC-loaded APCs augment antitumor immunity of exhausted CD8 T cells *in vivo*.

To explore whether the enhanced anti-tumor activity induced by αGC-loaded APCs in the anti-PD-1-resistant tumor model was due to the reinvigoration of tumor antigen-specific exhausted CD8 T cells, I utilized the OT-I TCR transgenic mouse system, in which most CD8 T cells recognize OVA antigenic peptide loaded onto MHC class I. A recent study demonstrated that eight days after transfer of *in vitro*-generated OT-I effector CD8 T cells (OT-I cells) into mice bearing B16-OVA, OT-I cells in the tumor environment produced few cytokines and were found to be exhausted (46). CD45.1^{+}OT-I cells which were activated with anti-CD3/anti-CD28 for 2 days and then expanded with low dose IL-2, were transferred into B16F10-OVA-bearing C57BL/6 mice **(Figure 10A)**. Flow cytometric analysis confirmed that all the effector OT-I cells expressed low levels of inhibitory receptors and high levels of CD44, indicating sufficient activation of the donor cells before transfer **(Figure 11A)**. αGC-loaded APCs were intravenously injected eight days after OT-I adoptive transfer when the transferred OT-I cells became exhausted, considering the high expression of PD-1, Tim3 and LAG3

(Figure 11B). I confirmed that the transferred OT- I cells had defects in producing effector molecules compared to effector OT- I cells upon restimulation with peptides **(Figure 11C)**. Treatment of αGC-loaded APCs resulted in delayed tumor growth, which was dependent on CD8 T cells **(Figure 10B)**. Two days after the administration of αGC-loaded APCs, tumor-infiltrating exhausted OT-I cells expanded and produced more effector molecules, such as IFNγ, TNFα, CD107a and granzyme B, than those in control APC-treated mice **(Figure 12A-B and 13A)**. In addition, the expression levels of T-bet, ki-67 and CD28 on tumor-infiltrating OT-I cells in αGC-loaded APC-treated mice were increased compared with those levels in the control APC-treated mice **(Figure 12C-D)**. I also observed that PD-1 expression in tumor-infiltrating OT-I cells was significantly down-regulated by αGC-loaded APC administration **(Figure 12C-D)**. Consistent with the phenotypic changes, the cytotoxicity of tumor-infiltrating OT-I cells against B16F10-OVA tumor cells was augmented by the treatment of αGC-loaded APCs **(Figure 13B)**. Taken together, these data indicate that treatment of αGC-loaded APCs enhanced anti-tumor immunity by restoring the polyfunctionality, proliferative capacity and cytotoxicity of the tumor antigen-specific CD8 T cells.

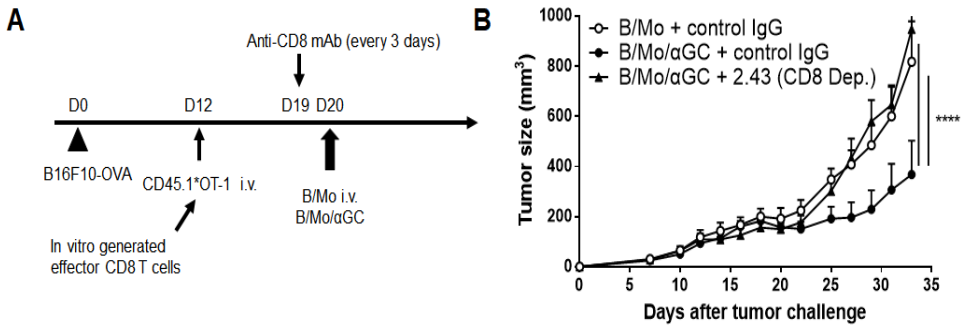

Figure 10. αGC-loaded APCs elicits antitumor immunity dependent on CD8 T cells.

(A) Experimental scheme. *In vitro*-generated effector congenic OT-I CD8 T cells were transferred into B16F10-OVA-bearing mice. B/Mo/αGC or their control B/Mo were injected 8 days after *in vivo* OT-I adoptive transfer. To deplete CD8 T cells, tumor-bearing mice were i.p. injected with anti-CD8 (2.43) every three days starting one day before the treatment of αGC-loaded APCs. **(B)** Tumor growth was measured three times weekly, and tumor sizes are presented as the means ± SEM. Data show one representative experiment (6-9 mice per group) out of two independent experiments. Statistical differences in tumor sizes were determined by two-way ANOVA with Bonferroni multiple comparison tests. (*, $P<0.05$; **, $P<0.01$; ***, $P<0.001$; ****, $P<0.0001$).

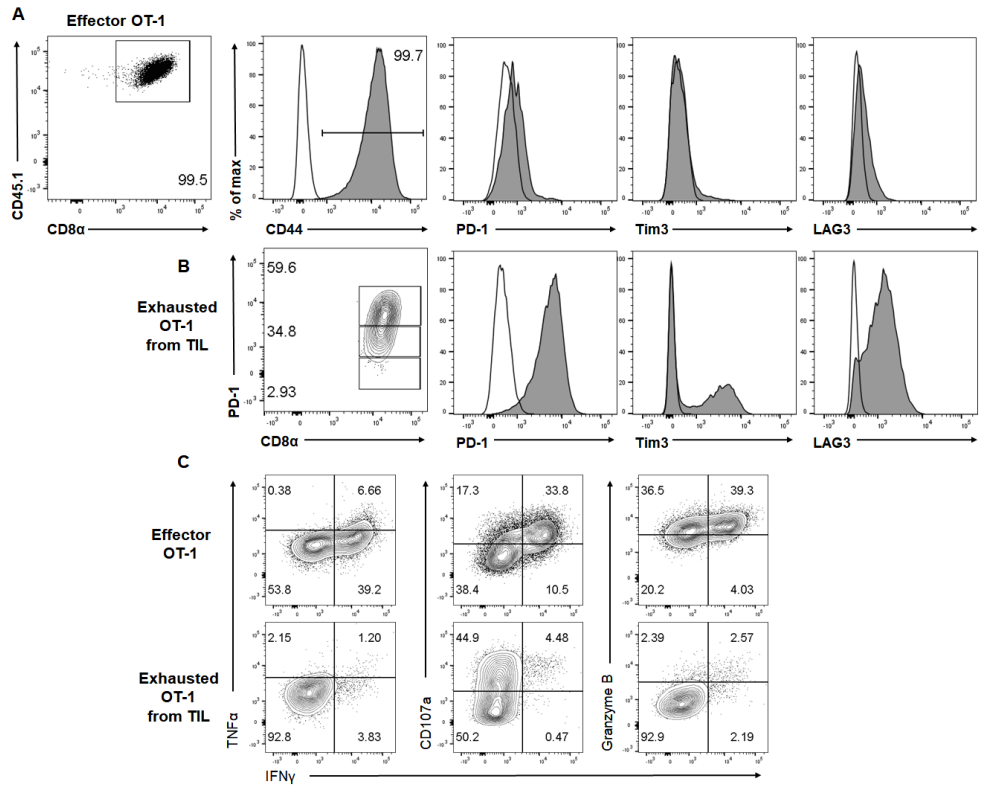

Figure 11. Phenotypic characterization of *in vitro*-generated effector OT-I cells and Ag-specific CD8 T cells in tumors.

(A) Total CD8 T cells isolated from congenic ($CD45.1^+$) OT-I mice by positive selection using anti-CD8 microbeads were activated by anti-CD3 and anti-CD28 (1 μg/mL) on pre-coated plates. From day 2, T cells were amplified with low dose recombinant IL-2 until day 5. CD44, PD-1, Tim-3 and LAG3 expression in $CD8\alpha^+CD45.1^+$ cells were analyzed by flow

cytometry (blank: isotype control). The data are representative of three independent experiments. **(B)** On day 8 after the transfer of effector OT-I cells generated as described in **(A)**, the cell surface expression of PD-1, Tim-3 and LAG3 in CD45.1^{+} Ag-specific CD8 T cells in the tumor was analyzed. **(C)** *In vitro*-generated effector OT-I cells or exhausted OT-I cells isolated from tumor tissues were restimulated with OT-I peptide and CD3-depleted APCs for 3 days. IFNγ expression was analyzed together with TNFα, CD107a, or granzyme B expression. The data are from one representative experiment out of two independent experiments.

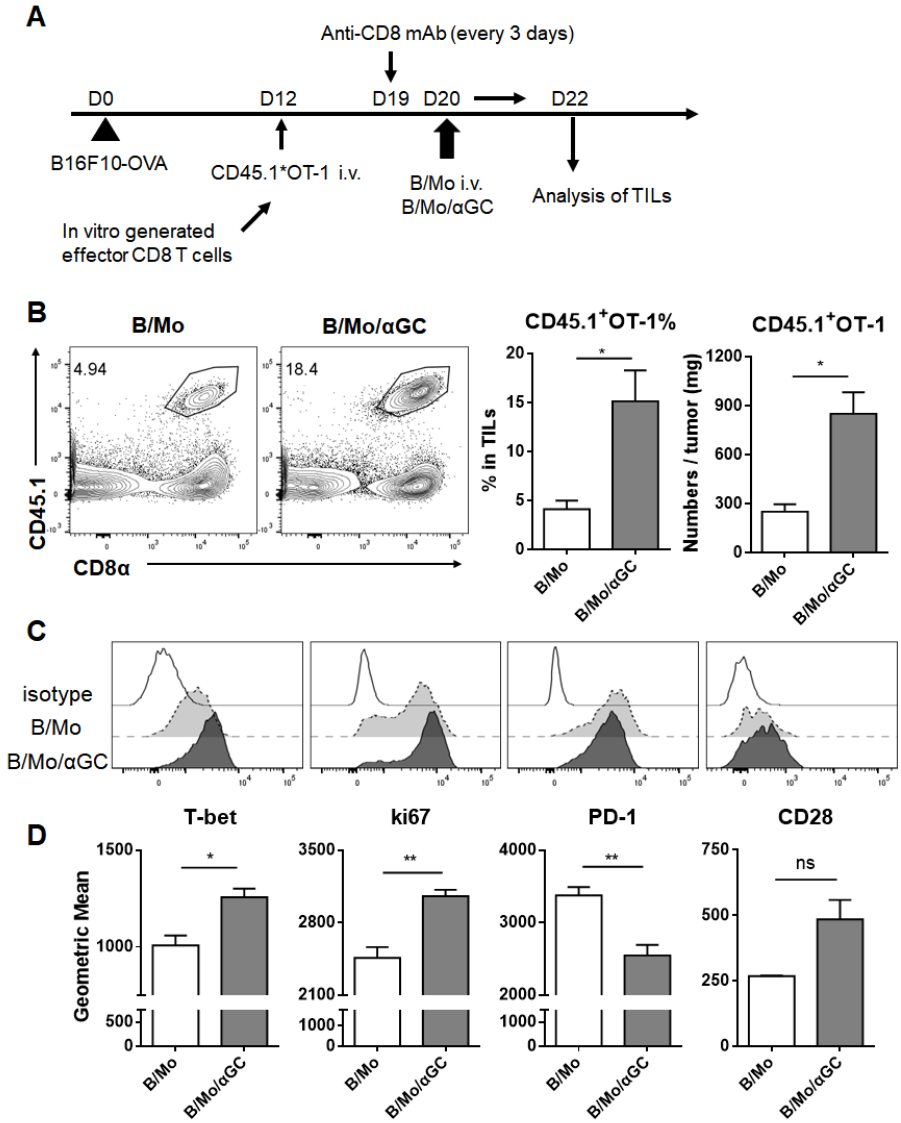

Figure 12. Administration of αGC-loaded APCs reinvigorates Ag-specific exhausted CD8 T cells.

(A) Experimental scheme. *In vitro*-generated effector congenic OT-I CD8 T cells were transferred into B16F10-OVA-bearing mice. B/Mo/αGC or their control B/Mo were injected 8 days after *in vivo* OT-I adoptive transfer. **(B-D)** TIL CD8 T cells were analyzed 2 days after the αGC-loaded APC transfer. **(B)** Representative flow cytometry plots are shown for Ag-specific CD8 T cells in tumors. The graphs show the frequency and quantification of Ag-specific CD45.1^{+}OT-I cells in TILs. **(C-D)** T-bet, Ki67, PD-1, and CD28 in CD45.1^{+} Ag-specific CD8 T cells were analyzed by flow cytometry. **(C)** Overlaid histogram plots are representative of three independent experiments (shaded histograms: control B/Mo treated group; filled histograms: αGC-loaded B/Mo treated group; open histograms: isotype control). **(D)** The mean fluorescence intensities (MFIs) of T-bet, Ki67, PD-1, and CD28 on the tumor-infiltrating congenic OT-I cells between vehicle and αGC-loaded APC-treated mice are shown. The data are presented as the means ± SEM and are representative of two or more independent experiments (n.s., nonsignificant; *, $P<0.05$; **, $P<0.01$).

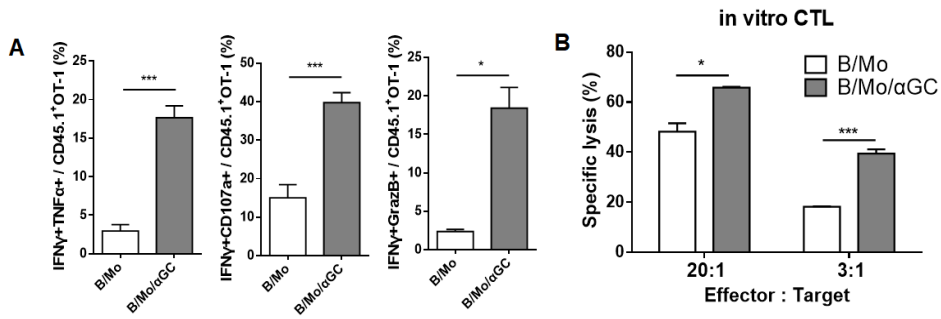

Figure 13. αGC-loaded APCs augment the antitumor immunity of Ag-specific exhausted CD8 T cells *in vivo*.

(A-B) TIL CD8 T cells were analyzed 2 days after the αGC-loaded APC transfer described in figure 12A. **(A)** Intracellular staining for the coproduction of IFNγ, TNFα, CD107a, and granzyme B upon the stimulation of TIL CD8 T cells with OT-I peptide. **(B)** Analysis of the cytotoxicity of Ag-specific CD8 T cells in tumors 2 days after the αGC-loaded APC treatment. ^{51}Cr-labeled B16F10-OVA tumor cells were used as target cells. The data are presented as the means ± SEM and representative of two independent experiments. The data in **(A–B)** were analyzed using an unpaired two-tailed Student's *t*-test (n.s., nonsignificant; *, P<0.05; **, P<0.01; ***, P<0.001; ****, P<0.0001).

Exhausted CD8 T cells in the tumor can be reinvigorated by αGC-induced cytokines.

Given that *i*NKT cells stimulated by αGC produce various cytokines, I hypothesized that cytokines induced by *i*NKT cell activation via αGC-loaded APC transfer might have affected exhausted CD8 T cells in the tumor environment. To identify the *i*NKT cell activation-induced cytokine(s) responsible for this effect, I obtained cytokine mixtures (αGC Supernatant; αGC Sup) by culturing total splenocytes with αGC for 24 h. Exhausted OT-I cells, isolated as described in figure 11A, were co-cultured with peptide and APCs in the presence of αGC Sup or control Sup for 3 days **(Figure 14A)**. In result, αGC Sup enhanced the Ag-specific expansion of exhausted OT-I cells compared with control Sup **(Figure 14B)**. αGC Sup-stimulated exhausted OT-I cells expressed higher level of effector molecules, including IFNγ, TNFα, CD107a and granzyme B than those of control Sup-treated cells **(Figure 14C)**. I observed a similar enhancement of effector functions of exhausted OT-I cells by treatment with the culture supernatant obtained from splenocytes stimulated with αGC-loaded APCs **(Figure 15A-B)**. Moreover, expression of T-bet and ki67 was elevated in αGC Sup-treated OT-I cells **(Figure 14D)**. CD28 expression was marginally increased by αGC Sup treatment compared with the control, while the PD-1 level was not

significantly changed. A recent study has demonstrated that CD8 T cells in tumors show two distinct chromatin states: $CD38^{low}CD101^{low}$ CD8 T cells are in a reversible dysfunctional state, whereas $CD38^{hi}CD101^{hi}$ CD8 T cells are in a fixed dysfunctional state that is resistant to reprogramming. Tumor-infiltrating $CD38^{hi}CD101^{hi}$ CD8 T cells exhibit a defect in regaining the ability to secrete cytokines even after exposure to IL-15, which can restore the function of $CD38^{low}CD101^{low}$ CD8 T cells (50). To delineate that this dichotomy could also be applied to the reinvigorating effect of αGC Sup, I sorted each $CD38^{hi}CD101^{hi}$ and $CD38^{low}CD101^{low}$ cells from the tumor and treated with αGC Sup in the *in vitro* restimulation experiment. Intriguingly, $CD38^{hi}CD101^{hi}$ as well as $CD38^{low}CD101^{low}$ exhausted OT-I cells were susceptible to αGC Sup-mediated reinvigoration of the effector function **(Figure 16A-B)**. Next, I examined which cytokines induced by αGC stimulation were involved in restoring CD8 T cell exhaustion. Using an *in vitro* cytokine-neutralizing system, I found that blockade of either IL-2 or IL-12 significantly abrogated the recovery of the expansion and effector molecule expression of exhausted OT-I cells induced by αGC Sup **(Figure 17A-C)**. These results indicate that *i*NKT stimulation by αGC restores the effector function of exhausted CD8 T cells via IL-2 and IL-12 induced by NKT cell activation.

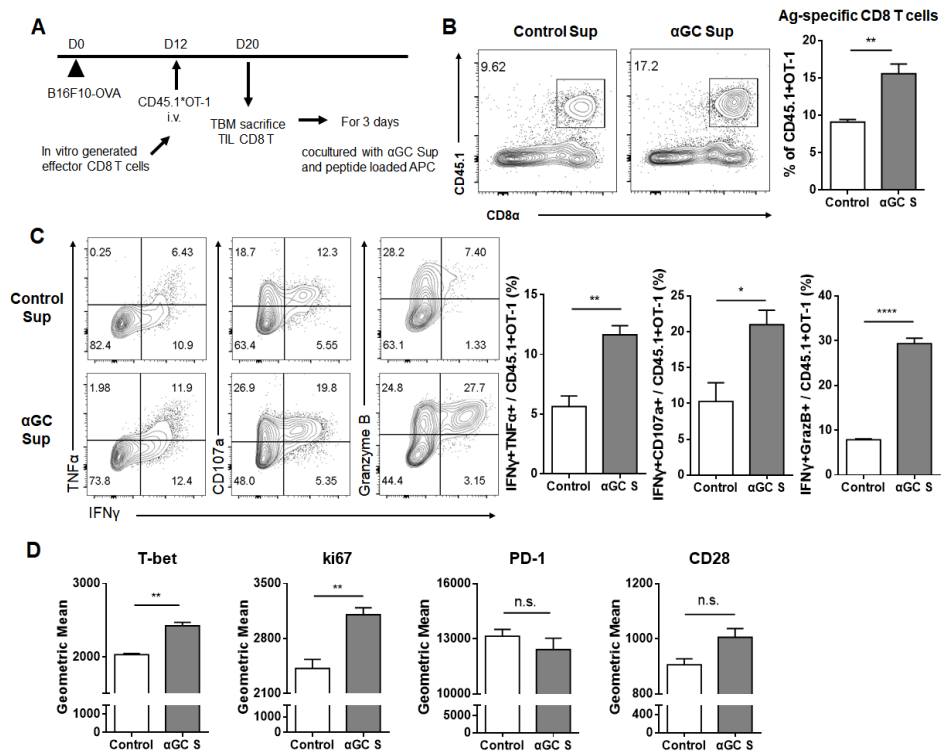

Figure 14. Exhausted CD8 T cells in tumors can be reinvigorated by αGC-induced cytokines.

(A) Experimental scheme. *In vitro*-generated effector congenic OT-I cells were transferred into B16F10-OVA bearing mice. Eight days after *in vivo* OT-I adoptive transfer, TIL CD8 T cells were isolated and restimulated with control or αGC Sup (αGC S) (50%), OT-I peptide, and CD3-depleted APCs for 3 days. **(B-C)** Representative flow cytometry plots are shown for Ag-specific CD8 T cells from tumors and intracellular cytokine staining for the

coproduction of IFNγ, TNFα, CD107a, and granzyme B. Graphs show a summary of the frequency of Ag-specific CD8 T cells and cytokine coproduction. **(D)** MFI of T-bet, ki67, PD-1, and CD28 on the tumor-infiltrating congenic OT-I cells between the control and αGC Sup-treated group are shown. **(B-D)** Statistical differences between the control and αGC Sup-treated group were determined using an unpaired two-tailed Student's *t*-test. Data in **(B-D)** are presented as the means ± SEM and are representative of three independent experiments (n.s., nonsignificant; *, P<0.05; **, P<0.01; ***, P<0.001; ****, P<0.0001).

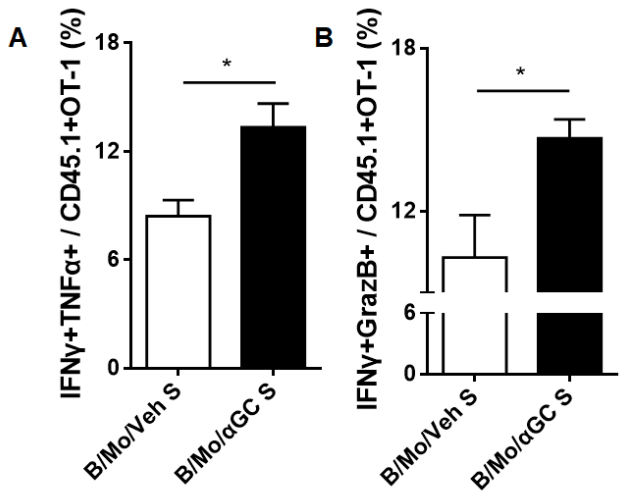

Figure 15. Soluble factors induced by B/Mo/αGC can enhance the effector function of exhausted tumor-specific CD8 T cells *in vitro*.

The experiments in figure 14 were recapitulated using B/Mo/αGC-stimulated culture supernatant (B/Mo/αGC S) instead of αGC-stimulated culture supernatant. Exhausted OT-I cells were restimulated with B/Mo culture supernatant (B/Mo S) or B/Mo/αGC culture supernatant (B/Mo/αGC S) in the presence of OT-I peptide and CD3-depleted APCs for 3 days. **(A-B)** The graphs show a summary of the frequencies of $IFN\gamma^+TNF\alpha^+$ cells and $IFN\gamma^+$granzyme B^+ cells. One representative experiment out of two is shown. Statistical differences between the control and B/Mo/αGC Sup-treated groups were determined using unpaired two-tailed Student's *t*-test (*, $P<0.05$).

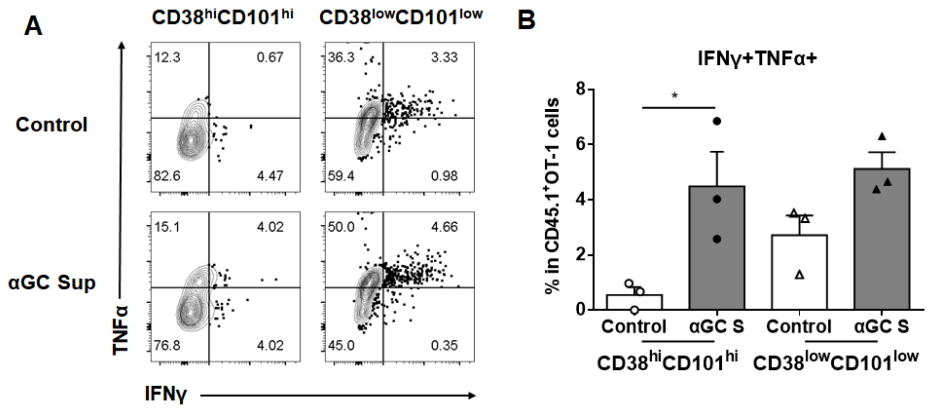

Figure 16. Ag-specific CD8 T cells in a fixed dysfunctional state can be reactivated by *i*NKT-ligand activation.

In the same system as that described in figure 14, CD8 T cells in tumor tissues were isolated from B16F10-OVA tumor-bearing mice by magnetic sorting. CD45.1^{+}OT-I cells were further sorted with CD38 and CD101 by FACS sorting. Cytokine production by sorted CD38^{low}CD101^{low} and CD38^{hi}CD101^{hi} CD8 T cells was analyzed after 3 days of stimulation with αGC Sup or control Sup in the presence of OT-I peptide-loaded APCs. **(A)** Representative flow cytometry plots for IFNγ and TNFα production in tumor antigen-specific CD8 T cells. **(B)** Summary of the frequency of IFNγ^{+}TNFα^{+} cells. The data show one representative experiment out of two independent experiments. Statistical differences between the control and αGC Sup-treated groups were determined using unpaired two-tailed Student's *t*-test (*, P<0.05).

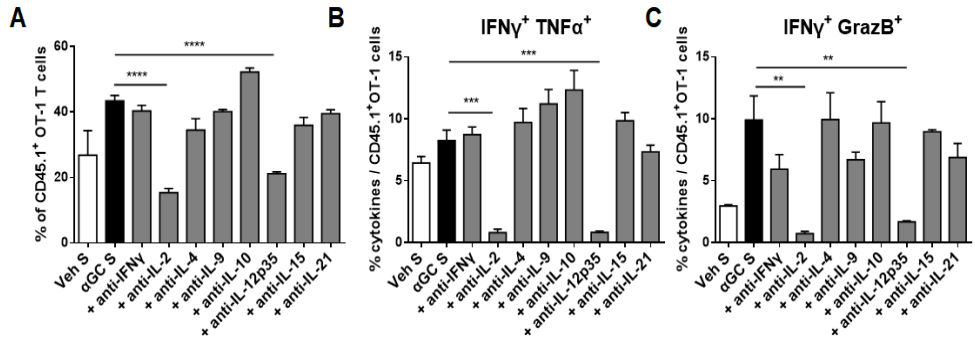

Figure 17. Exhausted CD8 T cells in tumors can be reinvigorated by αGC-induced cytokines dependent on IL-2 and IL-12.

In the same system as that described in figure 14A, to neutralize cytokines *in vitro*, the indicated antibodies (10 µg/mL) were added in the αGC Sup-treated group during restimulation for 3 days. The frequency of Ag-specific CD8 T cells and cytokine coproduction were analyzed by flow cytometry. Statistical differences between the αGC Sup-treated group with or without cytokine neutralization were determined using two-way ANOVA with Bonferroni multiple comparison tests. Data in **(A-C)** are presented as the means ± SEM and are representative of three independent experiments (n.s., nonsignificant; *, P<0.05; **, P<0.01; ***, P<0.001; ****, P<0.0001).

IL-2 and IL-12 induced by αGC-loaded APCs promote anti-tumor immunity *in vivo*.

Having confirmed that IL-2 and IL-12 induced by αGC stimulation were responsible for the restoration of exhausted CD8 T cells *in vitro,* I analyzed the cellular sources of IL-2 and IL-12 after the administration of αGC-loaded APCs by flow cytometry. I found that splenic *i*NKT cells mainly produced IL-2, while both $CD11c^+$ dendritic cells and $CD11b^+$ myeloid cells contributed to IL-12 production by splenocytes **(Figure 18A-B)**. I sought to evaluate whether these cytokines were also attributed to enhanced anti-tumor activity by αGC-loaded APCs. To achieve this goal, tumor-bearing mice were treated with anti-IL-2 and/or anti-IL-12p40 neutralizing mAbs concomitant with the αGC-loaded APC treatment. Administration of either anti-IL-2 or anti-IL-12p40 completely abrogated αGC-loaded APC-mediated regression of tumor growth, suggesting that both IL-2 and IL-12 contributed to the anti-tumor effect of the αGC-loaded APC treatment **(Figure 19A-B)**.

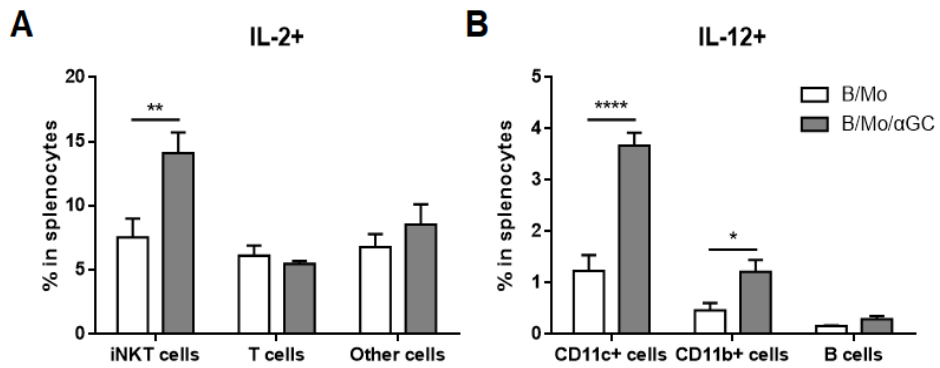

Figure 18. Cellular source of IL-2 and IL-12 after administration of αGC-loaded APCs.

(A-B) IL-2 production by *i*NKT cells, T cells and $CD3^-$ non-T cells and IL-12 production by $CD11c^+$, $CD11b^+$ and B cells within the splenocytes isolated from B16F10-OVA tumor-bearing mice were analyzed 6 h after αGC-loaded APC treatment. Statistical differences were determined by two-way ANOVA with Bonferroni multiple comparison tests (*, $P<0.05$; **, $P<0.01$; ***, $P<0.001$; ****, $P<0.0001$).

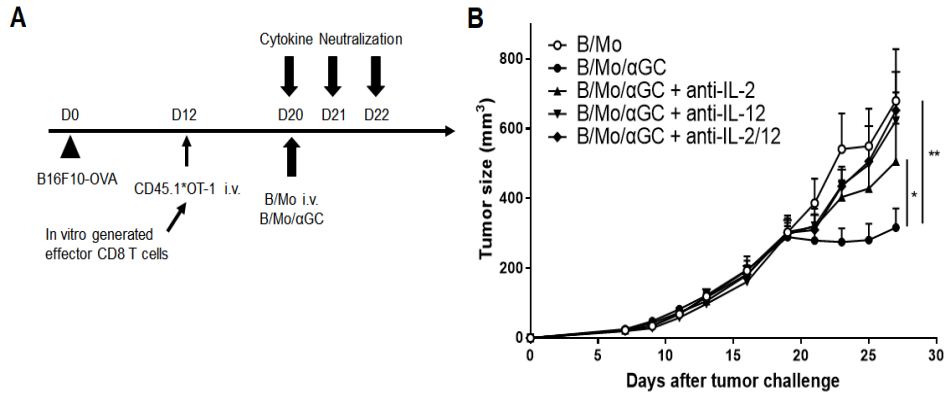

Figure 19. The anti-tumor effect of αGC-loaded APCs is dependent on IL-2 and IL-12.

(A-B) *In vitro*-generated effector congenic OT-I cells were transferred into B16F10-OVA-bearing mice. Eight days after *in vivo* OT-I adoptive transfer, αGC-loaded APCs (B/Mo/αGC) or their control B/Mo were injected. To neutralize IL-2 and IL-12, anti-IL-2 (JES6-5H4), anti-IL-12p40 (C17.8) or both were i.p. administered (1 mg/mouse) 2 h before the B/Mo/αGC transfer and then 24 and 48 h after the first injection (500 µg/mouse). **(B)** Tumor growth was measured three times weekly, and tumor sizes are presented as the means ± SEM. Statistical differences were determined by two-way ANOVA with Bonferroni multiple comparison tests (*, $P<0.05$; **, $P<0.01$).

Combined therapy with anti-PD-1 blockade and αGC-loaded APC treatment

I next investigated the therapeutic efficacy of anti-PD-1 therapy was enhanced when combined with αGC-loaded APCs in the anti-PD-1-resistant tumor model **(Figure 20A)**. As I demonstrated earlier, although tumor-bearing mice were refractory to four times of anti-PD-1 treatment from day 13 after tumor inoculation, αGC-loaded APCs substantially suppressed tumor growth if administered twice at day 13 and six days later. Importantly, the combination of αGC-loaded APCs with anti-PD-1 completely eradicated the tumors and prolonged overall survival of tumor-bearing mice. The anti-tumor effect of combination therapy was dependent on CD8 T cells, as shown that this effect was almost completely abrogated by CD8 T cell depletion **(Figure 20B-C)**. In the MC38 tumor model, the combination of αGC-loaded APCs with anti-PD-1 also inhibited tumor growth more effectively than treatment with αGC-loaded APCs alone **(Figure 21)**. Altogether, these results indicate that the combination of αGC-loaded APCs and PD-1 blockade elicits strong CD8 T cell-dependent anti-tumor responses.

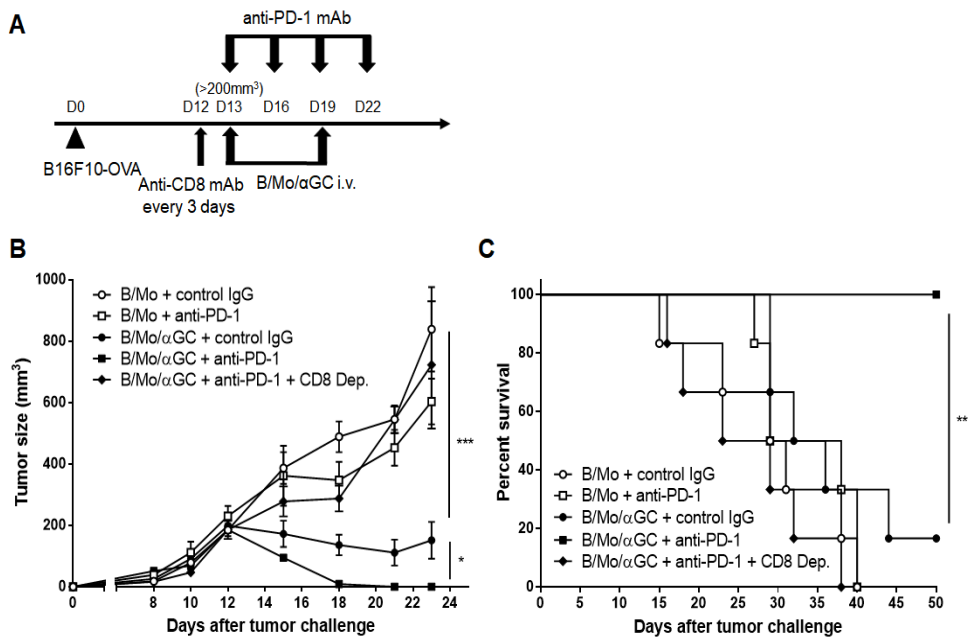

Figure 20. Combined therapy with anti-PD-1 blockade and αGC-loaded APCs.

(A-C) B16F10-OVA-bearing mice were treated with control IgG or anti-PD-1 on days 13, 16, 19, and 22 (starting when the tumor size exceeded over 200 mm^3). They were co-administered with B/Mo/αGC or control B/Mo on days 13 and 19. To deplete CD8 T cells, tumor-bearing mice were i.p. injected with anti-CD8 (2.43) every three days, starting on day 12. **(B)** Tumor growth was measured three times weekly, and tumor sizes are presented as the means ± SEM. Statistical differences in tumor sizes were determined by two-way

ANOVA with Bonferroni multiple comparison tests. **(C)** Survival curves from the data in **(B)**. The data included five to six mice per group. Comparisons were performed using the log-rank (Mantel-Cox) test (*, $P<0.05$; **, $P<0.01$; ***, $P<0.001$).

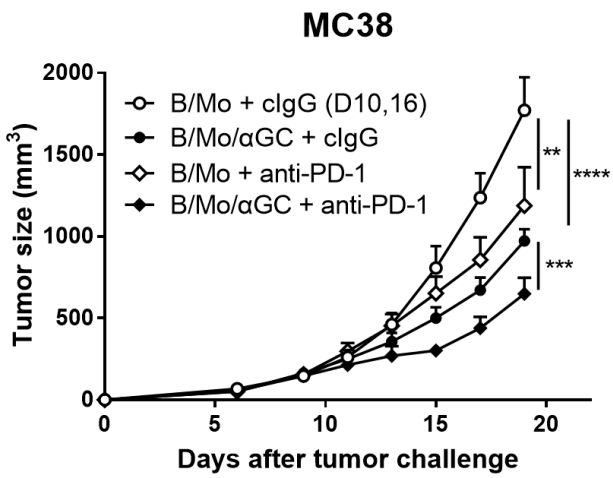

Figure 21. Administration of αGC-loaded APCs combined with anti-PD-1 enhances antitumor immunity in the MC38 tumor model.

C57BL/6 mice were s.c. injected with MC38 tumor cells (3.0×10^5). After 10 days, when the average tumor size was approximately 200 mm^3, treatments began. Tumor-bearing mice were treated with 300 μg of control IgG or anti-PD-1 on days 10, 13, 16, and 19 and injected with B/Mo or B/Mo/αGC (2.0×10^6 each) on days 10 and 16. Tumor sizes were measured three times weekly and are presented as the means ± SEM. The data show one representative experiment (4-6 mice per group) out of two independent experiments. Statistical differences in tumor sizes were determined by two-way ANOVA with Bonferroni multiple comparison tests (*, $P<0.05$; **, $P<0.01$; ***, $P<0.001$; ****, $P<0.0001$).

IL-2 and IL-12 also increase the effector function of tumor-infiltrating CD8 T cells in cancer patients.

I next investigated whether the effector function of human tumor-infiltrating lymphocyte (TIL) CD8 T cells could be enhanced by the cytokines induced by *i*NKT cell stimulation. To this end, culture supernatants were prepared by stimulating *i*NKT cells among PBMCs isolated from healthy subjects with αGC-loaded APCs for 24 h. When TILs isolated from colorectal cancer patients **(Table 1)** were stimulated with the αGC-treated culture supernatant, the frequency of $IFN\gamma^{+}TNF\alpha^{+}$ effector CD8 T cells was significantly increased compared to that in the controls **(Figure 22A-B)**. To directly test whether the two cytokines identified from the mouse models were also involved in the reinvigorating effect of the αGC-treated culture supernatant, the effector function of TIL CD8 T cells was examined after treatment with rhIL-2, rhIL-12 or both. Consistent with the conclusion in mouse studies, either rhIL-2 or rhIL-12 significantly increased the frequency of $IFN\gamma^{+}TFN\alpha^{+}$ cells among TIL CD8 T cells compared to that in the PBS controls **(Figure 23A-B)**. While the addition of rhIL-12 partially increased TNFα-producing cells among TIL CD8 T cells, rhIL-2 significantly induced both IFNγ- and TNFα-producing TIL CD8 T cells **(Figure 23C)**. I observed little if any additive effect induced by the combination of rhIL-2 and rhIL-12.

These results suggest that *i*NKT cell activation can contribute to the reinvigoration of human tumor-infiltrating exhausted CD8 T cells via the actions of IL-2 and IL-12.

Patient No.	AJCC7T	AJCC7N	AJCC7M	AJCC7stage
1	3	0	0	IIA
2	3	1a	0	IIIB
3	2	0	0	I
4	3	2a	1	IVA
5	3	0	0	IIA
6	3	2a	0	IIIB
7	3	1a	0	IIIB
8	3	0	0	IIA
9	3	0	0	IIA
10	2	1c	0	IIIA
11	3	0	0	IIA

Table 1. Clinical stages of the colorectal cancer patients. Colorectal cancer is classified by the criteria of AJCC (American Joint Committee on Cancer). Tumor (T) is used for describing size of the primary tumor. T1< means that the tumor has grown more than submucosa. T2 or T3 indicates that the tumor has grown into the muscularis propria or subserosa respectively. Node (N) indicates the number of tumor cells found in lymph nodes. Metastasis (M) means the stage of metastasis. Cancer stage is graded by combining the (T), (N), and (M) classifications.

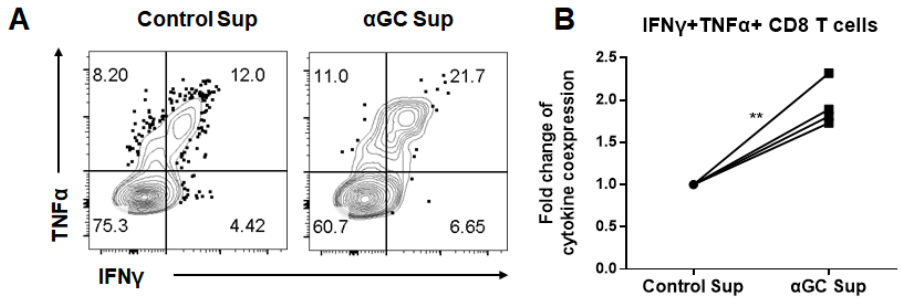

Figure 22. Soluble factors induced by αGC-loaded APCs enhance the effector function of tumor-infiltrating CD8 T cells in cancer patients.

(A-B) TILs isolated from patient tumors were treated with control or human αGC Sup (αGC S) overnight. Production of IFNγ and/or TNFα by CD8 TILs upon anti-CD3 stimulation (1 µg/mL) for 5 h, in the presence of the protein transport inhibitor brefeldin A and monensin during the last 4 h. **(A)** Representative flow cytometry plots showing the coproduction of IFNγ and/or TNFα by human αGC Sup. **(B)** Arbitrary units of the percentages of $IFN\gamma^{+}TNF\alpha^{+}$ cells in TIL CD8 T cells are depicted using fold change normalized by control Sup-treated samples. The values determined for individual patients are depicted. Data in **(B)** were analyzed using two-tailed paired *t*-test (n.s., nonsignificant; *, P<0.05; **, P<0.01).

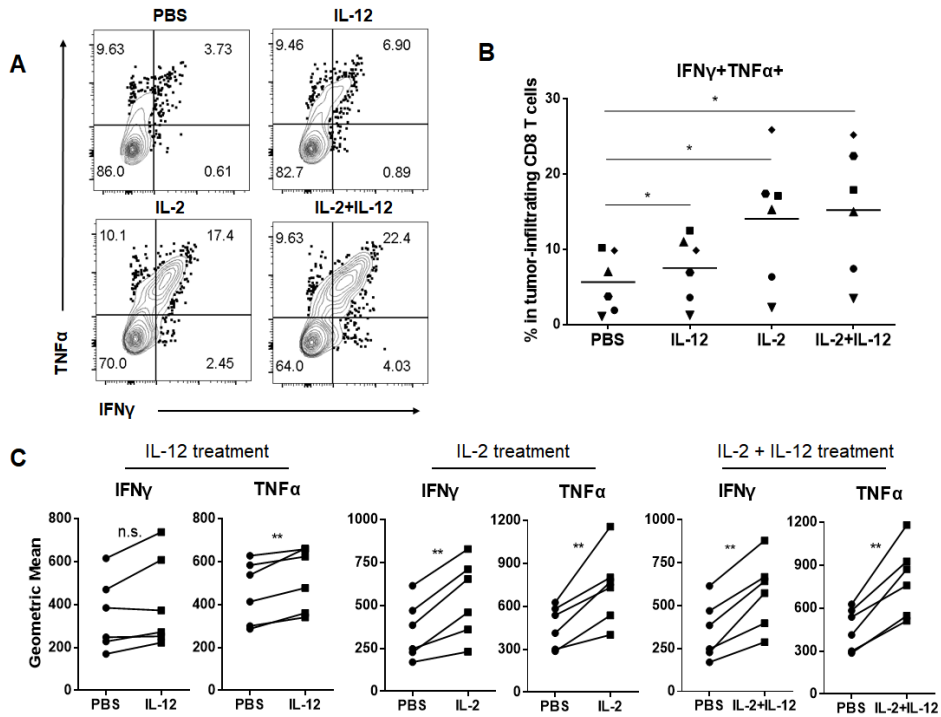

Figure 23. IL-2 and IL-12 increase the effector function of tumor-infiltrating CD8 T cells in cancer patients.

(A-C) TILs isolated from patient tumors were treated with control PBS, IL-2 (10 ng/mL), IL-12 (10 ng/mL), and IL-2 plus IL-12 overnight. Production of IFNγ and/or TNFα by CD8 TILs upon anti-CD3 stimulation (1 µg/mL) for 5 h, in the presence of the protein transport inhibitor brefeldin A and monensin during the last 4 h. **(A)** Representative flow cytometry plots showing the coproduction of IFNγ and/or TNFα by the indicated cytokines. **(B)** Data showing the percentages of $IFN\gamma^{+}TNF\alpha^{+}$ cells in TIL CD8 T cells are depicted. **(C)** The plots depict the

MFI of IFNγ or TNFα from CD8 T cells in tumors, by the addition of the indicated cytokines. The values determined for individual patients are depicted, and the lines in **(B)** denote the means. Data in **(B-C)** were analyzed using two-tailed paired *t*-test (n.s., nonsignificant; *, P<0.05; **, P<0.01).

Discussion

Despite the recent success of using an anti-PD-1 antibody as front-line therapy against advanced cancers, more than half of cancer patients tested in clinical trials remained refractory to the therapy (9). To improve the clinical outcomes of anti-PD-1 therapy, many combination strategies are under development (13). One of the main goals of combination therapies is overcoming the unresponsiveness of exhausted CD8 T cells in the tumor to anti-PD-1 therapy. Here, I found that *i*NKT cell activation by cell-associated αGC could inhibit the progression of anti-PD-1-resistant tumors by restoring the effector function of exhausted CD8 T cells in tumors. I also revealed that IL-2 and IL-12 produced after *i*NKT cell activation were the main components that reinvigorated exhausted CD8 T cells **(Figure 24)**. While activated *i*NKT cells were a main producer of IL-2, IL-12 was primarily produced by dendritic cells and myeloid cells. It seems that IL-12 induction in APCs in this experimental setting could have been attributed to IFNγ produced by either activated *i*NKT cells or transactivated NK cells (26,51).

The functional relevance of IL-2 and IL-12 in reinvigorating exhausted CD8 T cells in tumor models corresponds well with earlier studies

that demonstrated similar effects of these cytokines on virus infection-induced exhausted T cells. A previous report showed that IL-2 enhanced proliferative potential and granzyme B production by virus-specific CD8 T cells in LCMV chronic infection models (18). Additionally, IL-12 but not type 1 IFN rescued the exhausted HBV-specific CD8 T cells by inducing down-regulation of PD-1 and up-regulation of T-bet (19). In agreement with these studies, I confirmed that the increased effector function and anti-tumor immunity of tumor-infiltrating exhausted CD8 T cells by αGC-loaded APC treatment was dependent on IL-2 and IL-12. In addition to these cytokines, IL-21 can also play a crucial role in the maintenance and polyfunctionality of exhausted CD8 T and NK cells (20,21,39). However, I could not find any role for IL-21 in the restoration of exhausted CD8 T cells following αGC treatment in this *in vitro* system, although further analyses in more physiologically relevant *in vivo* settings are warranted.

A recent study demonstrated that exhausted CD8 T cells gradually up-regulated the expression of CD38 and CD101 with fixed chromatin states, which was associated with their rigid dysfunctional status (50). In that study, the effector function of $CD38^{hi}CD101^{hi}$ CD8 T cells was not reversed by IL-15, a cytokine known to enhance effector functions of tolerant CD8 T cells in

tumor models (22,50). Although my data showed that αGC-induced cytokines could partially enhance IFNγ and TNFα production by $CD38^{hi}CD101^{hi}$ CD8 T cells, it remains unclear whether they influence chromatin states. Blocking PD-1 signaling reinvigorates exhausted CD8 T cells in LCMV infection models, while the epigenetic fate of T cells is not significantly affected (52). In addition, patterns of chromatin accessibility of exhausted CD8 T cells are only slightly changed by anti-PD-L1 treatment in tumor-bearing mice (46). Therefore, further studies are needed to examine whether cytokines induced by αGC can change the chromatin states of exhausted CD8 T cells.

Previous studies have identified $PD\text{-}1^{hi}$ and $PD\text{-}1^{int}$ subsets of exhausted CD8 T cells in chronic viral infection models (53). PD-L1 blockade reduces spontaneous apoptosis and enhances the expansion and protective immunity of $PD\text{-}1^{int}$ CD8 T cells only (53). CD8 T cells marked with a transcriptional profile of $T\text{-}bet^{hi}$ ($PD\text{-}1^{int}$) represent the progenitor T cell subset and are ultimately converted to $Eomes^{hi}$ ($PD\text{-}1^{hi}$) CD8 T cells, which represent the terminally differentiated effector progeny (54). My data confirmed the down-regulation of PD-1 and increase in T-bet on tumor-infiltrating, Ag-specific exhausted CD8 T cells in αGC-loaded APC-treated mice, which might be one of the mechanisms by which αGC-loaded APCs

overcome the exhausted phenotype of CD8 T cells. In addition, recent studies have shown that CD40 stimulation by agonistic Ab can overcome resistance to anti-PD-1 therapy by converting PD-1^{hi} T cells into PD-1^{low} T cells (55). Furthermore, CD28 co-stimulation is also required for the effectiveness of anti-PD-1 therapy (17). My results showed that the administration of αGC-loaded APCs induced the down-regulation of PD-1 and up-regulation of CD28 on Ag-specific exhausted CD8 T cells in tumors, and these phenotypic changes might provide the rationale for the ability of PD-1 blockade to enhance the anti-tumor effect of αGC-loaded APC treatment.

Administration of αGC is known to induce *i*NKT cell anergy by triggering the up-regulation of PD-1 on *i*NKT cells (56). We and others have previously demonstrated that blocking the PD-1/PD-L1 interaction can prevent anergy induction in *i*NKT cells and enhance the antitumor effects of *i*NKT cells (56-58). In advanced tumors, NK cells also express Tim-3 and PD-1 and become functionally exhausted (39). In this regard, αGC-loaded APCs in combination with PD-1 blockade may have effects on exhausted NK cells and anergic *i*NKT cells, as well as exhausted CD8 T cells (40). Although the administration of αGC-loaded APCs could reverse the exhausted phenotype of CD8 T cells, it was not sufficient to completely reject the tumor

mass. Thus, I suggest that combined therapy between αGC-loaded APCs and PD-1 blockades not only reinvigorates exhausted CD8 T cells but also boosts diverse effector arms of antitumor immunity.

This is the first report to demonstrate that the cytokines induced by αGC can restore the anti-tumor effector function of exhausted CD8 T cells in anti-PD-1 resistant mouse tumor models. Among the cytokines, IL-2 and IL-12 are crucial for enhancing cytokine production by exhausted CD8 T cells in tumor-bearing mice and in cancer patients. Furthermore, I have clearly shown the synergism of the anti-tumor effect between αGC-loaded APC treatment and PD-1 blockade. Therefore, my study provides evidence for the application of cell-associated αGC as an adjuvant in anti-PD-1 therapy for cancer patients.

Summary

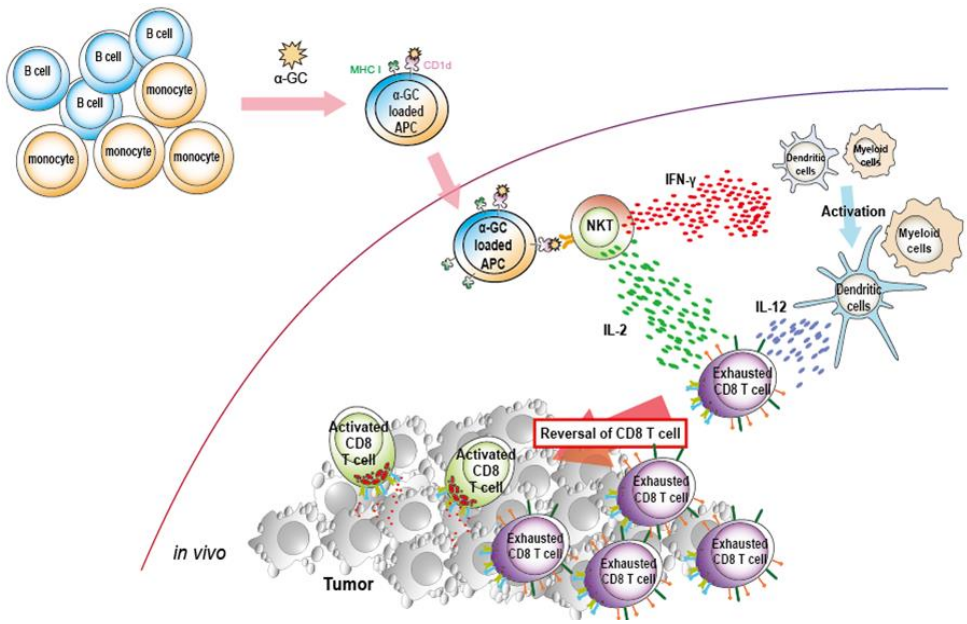

Figure 24. Graphical summary of this study: IL-2 and IL-12 induced by the administration of αGC-loaded APCs mediated reversal of exhausted CD8 T cell facilitates anti-tumor immunity. In this study, B cells and monocytes loaded with αGC (αGC-loaded APC) were administered into tumor-bearing mice. αGC-loaded APC could stimulate *i*NKT cells *in vivo* and activated *i*NKT cells in spleen secrete various cytokines. IL-2 produced by *i*NKT cells and IL-12 secreted by $CD11c^+$ dendritic cells and $CD11b^+$ myeloid cells reinvigorate tumor-infiltrating exhausted CD8 T cells and enhance the anti-tumor immunity.

References

1. Chen DS, Mellman I. Oncology meets immunology: the cancer-immunity cycle. Immunity **2013**;39:1-10
2. Wherry EJ. T cell exhaustion. Nature immunology **2011**;12:492
3. Schietinger A, Greenberg PD. Tolerance and exhaustion: defining mechanisms of T cell dysfunction. Trends in immunology **2014**;35:51-60
4. Wherry EJ, Kurachi M. Molecular and cellular insights into T cell exhaustion. Nature Reviews Immunology **2015**;15:486
5. Sakuishi K, Apetoh L, Sullivan JM, Blazar BR, Kuchroo VK, Anderson AC. Targeting Tim-3 and PD-1 pathways to reverse T cell exhaustion and restore anti-tumor immunity. Journal of Experimental Medicine **2010**;207:2187-94
6. Pardoll DM. The blockade of immune checkpoints in cancer immunotherapy. Nature Reviews Cancer **2012**;12:252
7. Apetoh L, Smyth MJ, Drake CG, Abastado J-P, Apte RN, Ayyoub M, *et al.* Consensus nomenclature for CD8+ T cell phenotypes in cancer. Oncoimmunology **2015**;4:e998538
8. Ott PA, Hodi FS, Robert C. CTLA-4 and PD-1/PD-L1 blockade: new immunotherapeutic modalities with durable clinical benefit in melanoma patients. AACR; 2013.
9. Topalian SL, Hodi FS, Brahmer JR, Gettinger SN, Smith DC, McDermott DF, *et al.* Safety, activity, and immune correlates of anti–PD-1 antibody in cancer. New England Journal of Medicine **2012**;366:2443-54

10. Hamid O, Robert C, Daud A, Hodi FS, Hwu W-J, Kefford R, *et al.* Safety and tumor responses with lambrolizumab (anti–PD-1) in melanoma. New England Journal of Medicine **2013**;369:134-44

11. Rizvi NA, Mazières J, Planchard D, Stinchcombe TE, Dy GK, Antonia SJ, *et al.* Activity and safety of nivolumab, an anti-PD-1 immune checkpoint inhibitor, for patients with advanced, refractory squamous non-small-cell lung cancer (CheckMate 063): a phase 2, single-arm trial. The Lancet Oncology **2015**;16:257-65

12. Wolchok JD, Kluger H, Callahan MK, Postow MA, Rizvi NA, Lesokhin AM, *et al.* Nivolumab plus ipilimumab in advanced melanoma. New England Journal of Medicine **2013**;369:122-33

13. Mahoney KM, Rennert PD, Freeman GJ. Combination cancer immunotherapy and new immunomodulatory targets. Nature reviews Drug discovery **2015**;14:561

14. Sharma P, Allison JP. Immune checkpoint targeting in cancer therapy: toward combination strategies with curative potential. Cell **2015**;161:205-14

15. Mescher MF, Curtsinger JM, Agarwal P, Casey KA, Gerner M, Hammerbeck CD, *et al.* Signals required for programming effector and memory development by CD8+ T cells. Immunological reviews **2006**;211:81-92

16. Kershaw MH, Westwood JA, Darcy PK. Gene-engineered T cells for cancer therapy. Nature Reviews Cancer **2013**;13:525

17. Kamphorst AO, Wieland A, Nasti T, Yang S, Zhang R, Barber DL, *et al.* Rescue of exhausted CD8 T cells by PD-1–targeted therapies is CD28-dependent. Science **2017**;355:1423-7

18. West EE, Jin H-T, Rasheed A-U, Penaloza-MacMaster P, Ha S-J, Tan WG, *et al.* PD-L1 blockade synergizes with IL-2 therapy in reinvigorating exhausted T cells. The Journal of clinical investigation **2013**;123:2604-15

19. Schurich A, Pallett LJ, Lubowiecki M, Singh HD, Gill US, Kennedy PT, *et al.* The third signal cytokine IL-12 rescues the anti-viral function of exhausted HBV-specific CD8 T cells. PLoS pathogens **2013**;9:e1003208

20. Elsaesser H, Sauer K, Brooks DG. IL-21 is required to control chronic viral infection. Science **2009**;324:1569-72

21. John SY, Du M, Zajac AJ. A vital role for interleukin-21 in the control of a chronic viral infection. Science **2009**;324:1572-6

22. Teague RM, Sather BD, Sacks JA, Huang MZ, Dossett ML, Morimoto J, *et al.* Interleukin-15 rescues tolerant CD8+ T cells for use in adoptive immunotherapy of established tumors. Nature medicine **2006**;12:335

23. Bendelac A, Savage PB, Teyton L. The biology of NKT cells. Annu Rev Immunol **2007**;25:297-336

24. Kronenberg M. Toward an understanding of NKT cell biology: progress and paradoxes. Annu Rev Immunol **2005**;26:877-900

25. Matsuda JL, Naidenko OV, Gapin L, Nakayama T, Taniguchi M, Wang C-R, *et al.* Tracking the response of natural killer T cells to a glycolipid antigen using CD1d tetramers. Journal of Experimental Medicine **2000**;192:741-54

26. Metelitsa LS, Naidenko OV, Kant A, Wu H-W, Loza MJ, Perussia B, *et al.* Human NKT cells mediate antitumor cytotoxicity directly by recognizing target cell CD1d with bound ligand or indirectly by producing IL-2 to activate NK cells. The Journal of Immunology **2001**;167:3114-22

27. Sag D, Krause P, Hedrick CC, Kronenberg M, Wingender G. IL-10–producing NKT10 cells are a distinct regulatory invariant NKT cell subset. The Journal of clinical investigation **2014**;124:3725-40

28. Coquet JM, Kyparissoudis K, Pellicci DG, Besra G, Berzins SP, Smyth MJ, *et al.* IL-21 is produced by NKT cells and modulates NKT cell activation and cytokine production. The Journal of Immunology **2007**;178:2827-34

29. Kumar A, Suryadevara N, Hill TM, Bezbradica JS, Van Kaer L, Joyce S. Natural Killer T Cells: an ecological evolutionary developmental biology perspective. Frontiers in immunology **2017**;8:1858

30. Kitamura H, Iwakabe K, Yahata T, Nishimura S-i, Ohta A, Ohmi Y, *et al.* The natural killer T (NKT) cell ligand α-galactosylceramide demonstrates its immunopotentiating effect by inducing interleukin (IL)-12 production by dendritic cells and IL-12 receptor expression on NKT cells. Journal of Experimental Medicine **1999**;189:1121-8

31. Tomura M, Yu W-G, Ahn H-J, Yamashita M, Yang Y-F, Ono S, *et al.* A novel function of Vα14+ CD4+ NKT cells: stimulation of IL-12 production by antigen-presenting cells in the innate immune system. The Journal of Immunology **1999**;163:93-101

32. Cui J, Shin T, Kawano T, Sato H, Kondo E, Toura I, *et al.* Requirement for Vα14 NKT cells in IL-12-mediated rejection of tumors. Science **1997**;278:1623-6

33. Nair S, Dhodapkar MV. Natural killer T cells in cancer immunotherapy. Frontiers in immunology **2017**;8:1178

34. Cerundolo V, Silk JD, Masri SH, Salio M. Harnessing invariant NKT cells in vaccination strategies. Nature Reviews Immunology **2009**;9:28

35. Fujii S-i, Shimizu K, Kronenberg M, Steinman RM. Prolonged IFN-γ–producing NKT response induced with α-galactosylceramide–loaded DCs. Nature immunology **2002**;3:867

36. Chung Y, Kim B-S, Kim Y-J, Ko H-J, Ko S-Y, Kim D-H, *et al.* CD1d-restricted T cells license B cells to generate long-lasting cytotoxic antitumor immunity in vivo. Cancer research **2006**;66:6843-50

37. Kim YJ, Ko HJ, Kim YS, Kim DH, Kang S, Kim JM, *et al.* α-Galactosylceramide-loaded, antigen-expressing B cells prime a wide spectrum of antitumor immunity. International journal of cancer **2008**;122:2774-83

38. Ko H-J, Lee J-M, Kim Y-J, Kim Y-S, Lee K-A, Kang C-Y. Immunosuppressive myeloid-derived suppressor cells can be converted into immunogenic APCs with the help of activated NKT cells: an alternative cell-based antitumor vaccine. The Journal of Immunology **2009**;182:1818-28

39. Seo H, Jeon I, Kim B-S, Park M, Bae E-A, Song B, *et al.* IL-21-mediated reversal of NK cell exhaustion facilitates anti-tumour immunity in MHC class I-deficient tumours. Nature Communications **2017**;8:15776

40. Seo H, Kim BS, Bae EA, Min BS, Han YD, Shin SJ, *et al.* IL21 Therapy Combined with PD-1 and Tim-3 Blockade Provides Enhanced NK Cell Antitumor Activity against MHC Class I-Deficient Tumors. Cancer Immunol Res **2018**;6:685-95

41. Lee KA, Bae EA, Song YC, Kim EK, Lee YS, Kim TG, *et al.* A multimeric carcinoembryonic antigen signal inhibits the activation of human T cells by a SHP-independent mechanism: A potential mechanism for tumor-mediated suppression of T-cell immunity. International journal of cancer **2015**;136:2579-87

42. Kamata T, Suzuki A, Mise N, Ihara F, Takami M, Makita Y, *et al.* Blockade of programmed death-1/programmed death ligand pathway enhances the antitumor immunity of human invariant natural killer T cells. Cancer Immunology, Immunotherapy **2016**;65:1477-89

43. Kim Y-J, Han S-H, Kang H-W, Lee J-M, Kim Y-S, Seo J-H, *et al.* NKT ligand-loaded, antigen-expressing B cells function as long-lasting antigen presenting cells in vivo. Cellular immunology **2011**;270:135-44

44. Kim E, Seo H, Chae M, Jeon I, Song B, Park Y, *et al.* Enhanced antitumor immunotherapeutic effect of B-cell-based vaccine transduced with modified adenoviral vector containing type 35 fiber structures. Gene therapy **2014**;21:106

45. Kim E-K, Jeon I, Seo H, Park Y-J, Song B, Lee K-A, *et al.* Tumor-derived osteopontin suppresses antitumor immunity by promoting extramedullary myelopoiesis. Cancer research **2014**

46. Mognol GP, Spreafico R, Wong V, Scott-Browne JP, Togher S, Hoffmann A, *et al.* Exhaustion-associated regulatory regions in CD8+ tumor-infiltrating T cells. Proceedings of the National Academy of Sciences **2017**;114:E2776-E85

47. Kim I-K, Kim B-S, Koh C-H, Seok J-W, Park J-S, Shin K-S, *et al.* Glucocorticoid-induced tumor necrosis factor receptor–related protein co-stimulation facilitates tumor regression by inducing IL-9–producing helper T cells. Nature medicine **2015**;21:1010

48. Lee KA, Shin KS, Kim GY, Song YC, Bae EA, Kim IK, *et al.* Characterization of age-associated exhausted CD8+ T cells defined by increased expression of Tim-3 and PD-1. Aging Cell **2016**;15:291-300

49. Juneja VR, McGuire KA, Manguso RT, LaFleur MW, Collins N, Haining WN, *et al.* PD-L1 on tumor cells is sufficient for immune evasion in immunogenic tumors and inhibits CD8 T cell cytotoxicity. Journal of Experimental Medicine **2017**:jem. 20160801

50. Philip M, Fairchild L, Sun L, Horste EL, Camara S, Shakiba M, *et al.* Chromatin states define tumour-specific T cell dysfunction and reprogramming. Nature **2017**;545:452

51. Yang Y-F, Tomura M, Ono S, Hamaoka T, Fujiwara H. Requirement for IFN-γ in IL-12 production induced by collaboration between Vα14+ NKT cells and antigen-presenting cells. International Immunology **2000**;12:1669-75

52. Pauken KE, Sammons MA, Odorizzi PM, Manne S, Godec J, Khan O, *et al.* Epigenetic stability of exhausted T cells limits durability of reinvigoration by PD-1 blockade. Science **2016**;354:1160-5

53. Blackburn SD, Shin H, Freeman GJ, Wherry EJ. Selective expansion of a subset of exhausted CD8 T cells by αPD-L1 blockade. Proceedings of the National Academy of Sciences **2008**;105:15016-21

54. Paley MA, Kroy DC, Odorizzi PM, Johnnidis JB, Dolfi DV, Barnett BE, *et al.* Progenitor and terminal subsets of CD8+ T cells cooperate to contain chronic viral infection. Science **2012**;338:1220-5

55. Ngiow SF, Young A, Blake SJ, Hill GR, Yagita H, Teng MW, *et al.* Agonistic CD40 mAb-driven IL12 reverses resistance to anti-PD1 in a T-cell–rich tumor. Cancer research **2016**;76:6266-77

56. Chang W-S, Kim J-Y, Kim Y-J, Kim Y-S, Lee J-M, Azuma M, *et al.* Cutting edge: Programmed death-1/programmed death ligand 1 interaction regulates the induction and maintenance of invariant NKT cell anergy. The Journal of Immunology **2008**;181:6707-10

57. Parekh VV, Lalani S, Kim S, Halder R, Azuma M, Yagita H, *et al.* PD-1/PD-L blockade prevents anergy induction and enhances the anti-tumor activities of glycolipid-activated invariant NKT cells. The Journal of Immunology **2009**;182:2816-26

58. Durgan K, Ali M, Warner P, Latchman YE. Targeting NKT cells and PD-L1 pathway results in augmented anti-tumor responses in a melanoma model. Cancer Immunology, Immunotherapy **2011**;60:547-58

국문 초록

면역관문 차단제를 이용한 항암면역치료법이 암환자를 치료하기 위한 새로운 효과적인 치료법으로 주목받고 있다. 특히 PD-1 차단제는 다양한 암 종의 후기 암환자에서 지속적인 항암효과를 나타내는 면역관문 차단제 중의 하나로 인정받고 있다. PD-1 차단제는 종양 미세환경에서 지속적인 암 항원의 자극에 의해 기능저하된(exhausted/dysfunctional) T 세포의 기능을 회복시켜 항암효과를 나타낸다고 알려져 있다. 그러나 면역관문차단제에 의해 항암효과를 나타내는 환자의 비율이 여전히 낮기 때문에 이를 최적화하기 위한 추가적인 연구가 필요한 상태이다.

본 연구에서는 PD-1 차단제에 저항성을 나타내는 마우스 종양 모델을 정립하고, PD-1 차단제에 반응성이 없는 것이 증가된 CD8 T 세포의 기능 저하와 연관이 있음을 보여주었다. 또한 자연살해 T 세포의 리간드인 α-galactosylceramide (αGC)를 이용하여 자연살해 T 세포를 활성화 시켰을 때 PD-1 차단제에 저항성을 나타내는 마우스 종양 모델에서 암 항원에 특이적인 기능저하 CD8 T

세포의 효과기 기능을 회복시켜 항암 효과를 유도함을 보여주었다. αGC 자극에 의해 생성된 사이토카인들 중에서 IL-2 와 IL-12 가 마우스 및 사람의 종양에 침윤된 기능저하 CD8 T 세포의 기능을 활성화 시키는데 중요하다는 것을 확인하였다. 추가적으로 αGC 를 적재한 항원제시세포와 PD-1 차단제의 병용 투여가 PD-1 차단제에 저항성을 나타내는 마우스 종양 모델에서 더욱 증대된 항암 효과를 나타냄을 확인할 수 있었다. 따라서 PD-1 차단제에 저항성이 있는 암 환자에서 자연살해 T 세포의 활성화법이 새로운 가능성 있는 암치료법으로 사용될 수 있다는 것을 밝힐 수 있었다.

주요어: CD8 T 세포 기능저하, 자연살해 T 세포, PD-1 차단제, IL-2, IL-12, 항암면역치료

학 번: 2012-22844